UMTRI-83-8

THE DYNAMIC BEHAVIOR OF NONUNIFORM TIRE/WHEEL ASSEMBLIES

Thomas D. Gillespie

November 1983

Technical Report Documentation Page

1. Report No.	2. Government Accession No.	3. Recipient's Catalog No.
UMTRI-83-8		

4. Title and Subtitle	5. Report Date
THE DYNAMIC BEHAVIOR OF NONUNIFORM TIRE/ WHEEL ASSEMBLIES	November 1983
	6. Performing Organization Code: 361858
7. Author(s): T.D. Gillespie	8. Performing Organization Report No.: UMTRI-83-8
9. Performing Organization Name and Address: The University of Michigan, Transportation Research Institute, 2901 Baxter Road, Ann Arbor, Michigan 48109	10. Work Unit No.
	11. Contract or Grant No.: MVMA Proj. 1162
12. Sponsoring Agency Name and Address: Motor Vehicle Manufacturers Association, 300 New Center Building, Detroit, Michigan 48202	13. Type of Report and Period Covered: Special
	14. Sponsoring Agency Code

15. Supplementary Notes

16. Abstract

Nonuniformities in the rotating tire and wheel components of a motor vehicle may excite ride vibrations. Both the vehicle and the wheel assembly are dynamic systems that interact via the forces and motions produced. Measurement of the force variations inherent to a nonuniform tire/wheel assembly in a meaningful way therefore requires a basic understanding of the dynamic systems involved.

Impedance methods are employed to formulate a dynamic model for a nonuniform tire/wheel assembly and a loading system that can represent either a test machine or a motor vehicle. The models are used to explain the potential error sources that may arise in tire uniformity tests on a machine that has dynamic response in the range of interest. The model of a vehicle coupled to a nonuniform tire/wheel assembly is used to explain the dynamic interaction that occurs between the vehicle and wheel assembly. Examples are given to illustrate the importance of impedance coupling in predicting the effect of nonuniformities on vehicle vibration.

17. Key Words	18. Distribution Statement
tire and wheel nonuniformities, tire uniformity, measurement, vehicle ride, dynamic modeling	UNLIMITED

19. Security Classif. (of this report)	20. Security Classif. (of this page)	21. No. of Pages	22. Price
NONE	NONE	53	

TABLE OF CONTENTS

1. INTRODUCTION. 1

2. DYNAMIC ANALYSIS. 4

2.1 Impedance Methods 4
2.2 Tire/Wheel Model. 8
2.3 Test Machine Model. 12

3. TIRE TEST MACHINE DYNAMIC EFFECTS 16

3.1 Calibration 17
3.2 Cross-Axis Dynamics 24
3.3 Summary of Machine Dynamic Interaction. 30

4. DYNAMIC INTERACTIONS ON A VEHICLE 33

4.1 Linear Model. 33
4.2 Examples of Wheel/Vehicle Dynamic Behavior. 37
4.3 Conclusions 49

5. REFERENCES. 51

1. INTRODUCTION

Tires and wheels, like any manufactured component, contain irregularities due to the practical limits of tolerances in the manufacturing process. Certain types of irregularities may result in mass imbalances or dimensional runouts. The combination of these effects in a tire/wheel assembly may excite vibrations on the vehicle on which the wheel is mounted.

Though irregularities in the individual components may be measured at the completion of the manufacturing process, the way in which they combine and interact with other components to excite vibrations in a motor vehicle is not well understood. Specifically, the tire/wheel assembly constitutes a multi-modal dynamic system, the behavior of which can only be predicted in a meaningful way through its coupling to a loading system. In the manufacturer's setting, the loading system may be one of many different types of test machines, which are dynamically quite different than a motor vehicle. The measurements obtained by the manufacturer therefore have an uncertain relationship to the dynamic effects that will be produced on any given vehicle.

Particularly within the tire industry, manufacturers often monitor the dimensional variations (free radial runout, lateral runout, and loaded radial runout), tire imbalance, and/or the force variations produced when the tire is rolled at constant radius against a drum (e.g., variations in radial, lateral, and tractive force). Various types of equipment are used for the measurement of force variations, and there is on-going concern with respect to (1) the comparison of measurements from different types of machines and (2) the disparity between force measurements on test machines and the dynamic forces produced on the vehicle.

In 1979, the Motor Vehicle Manufacturers Association (MVMA) initiated a research program to examine nonuniformities in truck tire/wheel assemblies that may act as sources of excitation to ride vibrations. Sharing a common interest, the Rubber Manufacturers Association (RMA), representing the tire manufacturing industry, has supported the research by providing a tire uniformity test machine for use in the research program.

The program, designated as the "Truck Tire/Wheel Systems Research Program," is organized into two phases. Phase I has the purpose of relating the common industry-measured forms of tire/wheel nonuniformities to the excitation forces they produce on the axles of heavy-duty commercial vehicles. Phase II has the purpose of developing methodology by which the tire/wheel assembly excitation forces are related to degradation in truck ride quality.

Given the interest in measuring the force variations produced by tire/wheel nonuniformities at high speeds (and hence high frequencies) in the Truck Tire/Wheel Systems Research Program being pursued at UMTRI, the understanding of dynamic behavior is particularly critical. The discussion in this report presents an analysis of the dynamic systems involved in the measurement of force variations exhibited by tire/wheel assemblies. The analysis is keyed toward a test machine with a dynamic configuration comparable to that of the MTS Systems, Inc. Model 860 Tire Test Machine shown in Figure 1 as installed at UMTRI for tire/wheel uniformity testing.

Of the many empirical and analytical aspects of the research, that dealing with the dynamic interactions of the tire/wheel assembly with either the vehicle or the test machine is perhaps the most complex. This report summarizes the analysis that has been performed in this program to provide a systematic understanding of the interactions involved. The report first describes methods for modeling the dynamic systems, then applies the models to explain (1) the potential dynamic interactions with uniformity test machines affecting the measurements obtained, and (2) the dynamic interactions with the vehicles affecting ride vibrations produced.

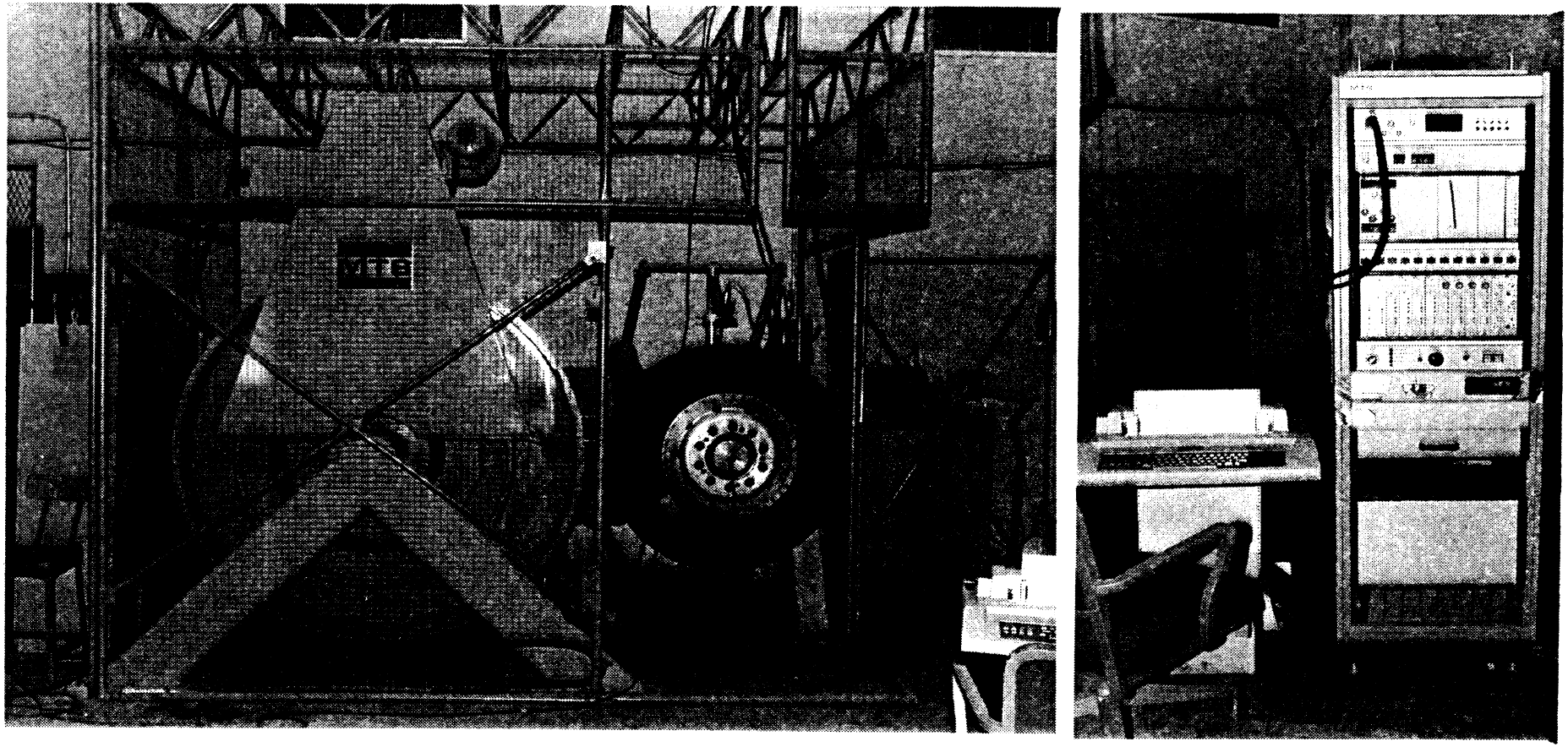

Figure 1. MTS Model 860 Tire Test Machine Installed at UMTRI.

2. DYNAMIC ANALYSIS

2.1 Impedance Methods

The dynamic behavior of mechanical systems is governed by Newton's laws of motion, normally written in differential equation form. The equations may be solved by a number of methods to determine how the system will behave; but for complicated dynamic systems the mathematical exercise may be quite lengthy.

For dynamic systems undergoing sinusoidal motions, shorthand methods can be used to reduce the mathematical complexity. The Impedance Method [1]* is one such shorthand method that allows the dynamic system to be described by simple algebraic equations. Thus, the emphasis can be placed on understanding the results with minimal distraction from the effort needed to follow complex mathematical manipulations. In this section, the Impedance Method will be explained and then applied to develop a dynamic model for the tire/wheel assembly. The analysis uses the "black box" concept in which dynamic systems are represented by the interrelated force and motion properties at one or two connection points. A further advantage of this method is that, in the case of complex systems for which analytical representation is impractical, physical measurements of impedance properties can be used to describe the system components in a quantitative manner.

The assumptions are made that the dynamic system has linear and bilateral (independent of direction) properties. Though real tires and vehicles depart somewhat from these assumptions, the linear analysis, nonetheless, provides a systematic understanding of the dynamic behavior adequate for the purposes of this report.

---

*Numbers in brackets indicate references in Section 5.

For a mechanical system, the impedance*, Z, is defined as the ratio of the driving force, F, to the resulting velocity, V, measured in the direction of force application. That is,

$$Z = F/V \tag{1}$$

If the velocity is measured at the point of force application, it is known as the "driving point" impedance. For example, if a radial force is applied at the contact patch of a tire and the radial velocity at that point is measured, the driving point impedance at the tire contact patch is obtained. If the driving force is applied at one point and the velocity is measured at another point, or in another direction, the "transfer" impedance is obtained. For example, the ratio of the radial force applied at the tire contact patch, to the velocity measured at the hub, is the tread-to-hub transfer impedance for the wheel. In general, the force and velocity are sinusoidal and are represented by complex numbers having amplitude and phase differences, thus the impedance is a complex quantity.

Note that although velocity is the measure of motion associated with impedance, it is directly related to displacement in sinusoidal motion. That is,

$$X = V/j\omega \tag{2}$$

where

X = displacement

j = $\sqrt{-1}$

ω = sinusoidal frequency

---

*The term "impedance" used with mechanical systems is analogous to its use in electrical theory, where it implies the complex resistance of a network which may contain capacitors or inductors as well as resistors. In the analogy, mechanical force is equivalent to voltage (electromotive force), and velocity is equivalent to current (flow rate of electrical charge).

Hence, the associated displacement is proportional to the velocity, divided by the frequency, and lags the velocity by a phase of 90 degrees. Thus, a dynamic system can be represented by its force-displacement rather than force-velocity (impedance) if desired. The force-displacement property is called the dynamic modulus*, D; i.e.,

$$D = F/X = j\omega\, F/V = j\omega\, Z \tag{3}$$

Inasmuch as the force-displacement properties of a tire/wheel assembly are more easily comprehended, this variable will be used in the subsequent analysis. In the modulus convention, the reader may note that spring, damping, and mass properties have the following representation:

Spring	$K = F/X = D_k$	$\therefore D_k = K$
Damping	$C = F/V = F/j\omega X = D_d/j\omega$	$\therefore D_d = j\omega C$
Mass	$M = F/\dot{V} = -F/\omega^2 X = -D_m/\omega^2$	$\therefore D_m = -\omega^2 M$

Note that the dynamic modulus can be envisioned as a stiffness function that may represent spring, damping, and mass properties and may vary in magnitude and phase as a function of frequency. For example, at low frequency, the modulus property of a tire may be close to constant, representing its radial stiffness property. At high frequency, it may increase with ω^2, representing the stiffness (or resistance) attributable to an inertial mass. And at other points, it may exhibit maxima or minima attributable to resonance or anti-resonance points of the dynamic system involved.

This method for modeling the dynamic properties of a tire/wheel assembly is not new, but has, for example, been used by other researchers [2,3,4]. Figure 2a shows the dynamic modulus at the tire contact patch

---

*The term "dynamic modulus" is commonly used in the textbooks to describe this property, although it is also sometimes called "dynamic stiffness." Likewise, the reciprocal property may be called "receptance" or compliance.

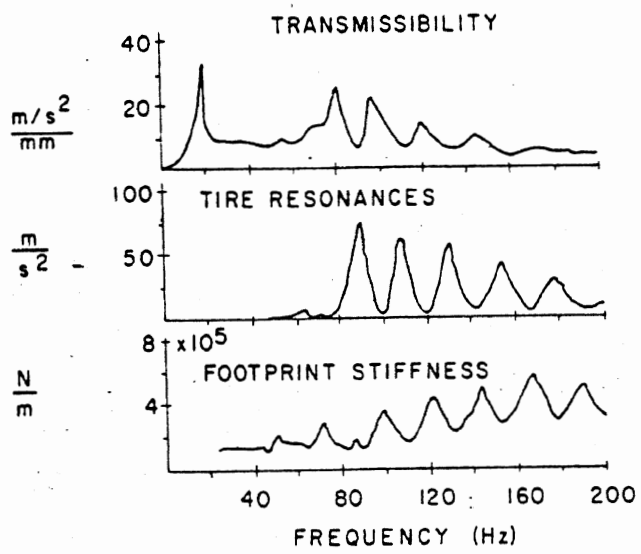

Figure 2a. Comparison of passenger car tire resonances with transmissibility and footprint stiffness results. [2]

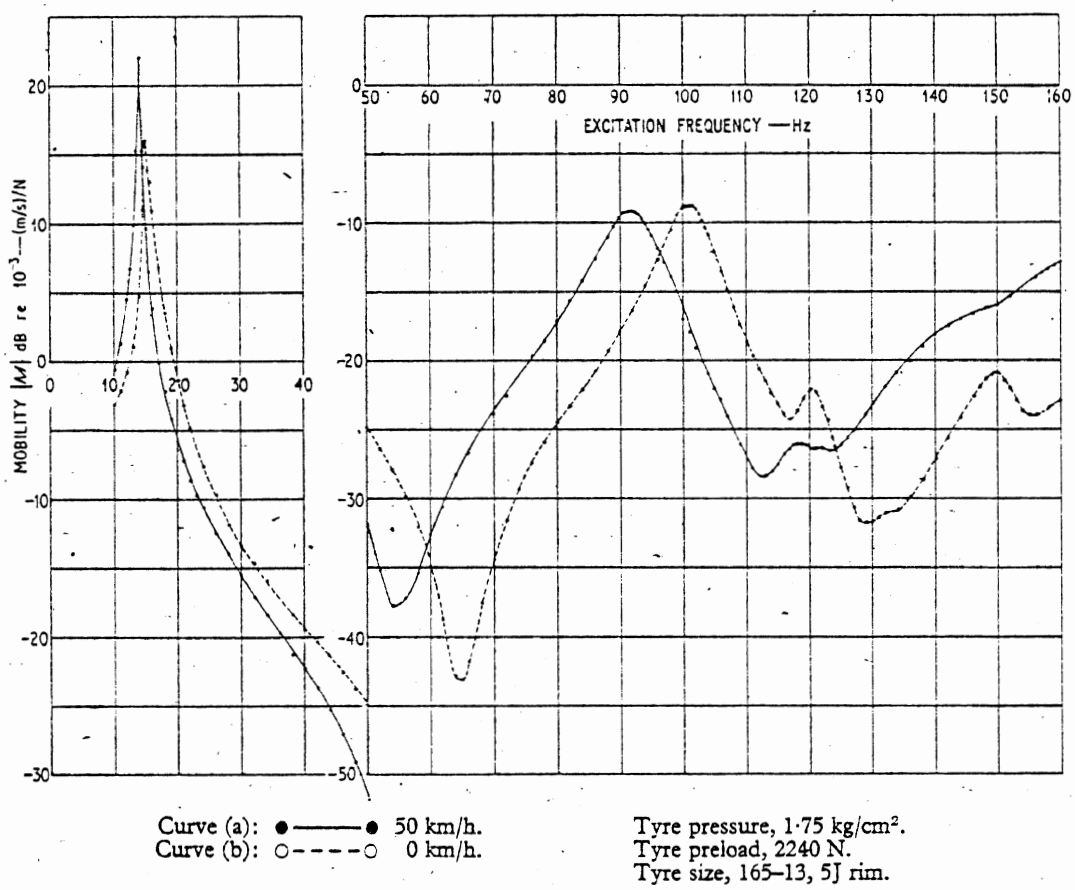

Figure 2b. The frequency variation of driving point mobility with rolling speed for radial ply passenger car tire. [4]

(footprint stiffness) measured under the front wheel of a passenger car; whereas Figure 2b shows the mobility (i.e., the inverse of impedance) measured at the spindle of a passenger car tire while rolled against a drum.

Perhaps the best appreciation for the dynamic properties can be gained by examining the footprint stiffness shown in Figure 2a. Note that in the range of 20-40 Hz, the stiffness is constant at a value of about 1.5×10^5 N/m (850 lb/in). In this range, which is above the axle resonance frequency, the spindle remains essentially motionless, and the stiffness measured is the radial spring rate of the tire. At higher frequencies, maxima and minima occur. The maxima (e.g., 100 Hz) occur at anti-resonant conditions in which the tire vibrates in a modal shape that is not symmetric about the wheel. As a consequence, it appears very stiff at the contact patch and accordingly acts to transmit the vibration input very directly to the wheel spindle [2]. Conversely, the minima (e.g., 90 Hz) represent symmetric vibration modes in which the tire is able to move freely with the input thus effectively absorbing those motions without transmitting them to the wheel.

2.2 Tire/Wheel Model

Nonuniformities in a tire/wheel assembly cause the forces to vary with the angle of rotation. The force variation repeats with each revolution and thus may be represented as the composite result of a series of sinusoidal harmonics [8]. In the case when the tire is in contact with a rigid drum or road surface, each harmonic may be represented either by a force generator in parallel with an impedance (Thevenin's Equivalent System) or a velocity generator in series with an internal impedance (Norton's Equivalent System). Both models are shown in Figure 3, with a dynamic modulus shown in lieu of an impedance and a displacement generator in lieu of a velocity generator. The output of the system is a force, F_h, and displacement, X_h, at the spindle on which the wheel is mounted. F_h is then equivalent to the cyclic force that would be imposed on the axle of a vehicle, while X_h represents any movement of the axle.

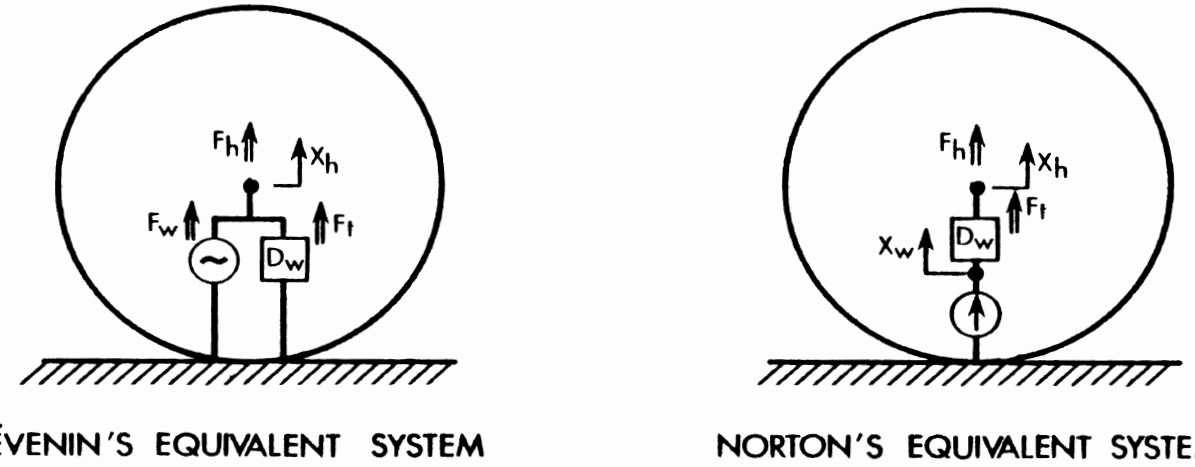

Figure 3. Dynamic models of a tire/wheel assembly with an internal nonuniformity.

The system equation is obtained by simply summing the forces at the spindle. Those forces are obviously F_w and F_h, but also include a contribution, F_t, from the modulus, D_w. Specifically, thinking of D_w as the stiffness of the tire, it is easy to see that:

$$F_t = D_w(X_{ground} - X_h) = D_w(0 - X_h) \tag{4a}$$

Therefore, the force at the hub is

$$F_h = F_w + F_t = F_w - D_w X_h \tag{4b}$$

Now if the spindle is absolutely rigid ($X_h = 0$),

$$F_h = F_w \tag{4c}$$

and the force developed at the spindle is equal to the nonuniformity force within the tire/wheel assembly. This is, in fact, the intent when force variations are measured.

On the other hand, if the force at the spindle is held constant (i.e., the force variation, F_h, equals zero), then the spindle must move according to the equation

$$X_h = F_w/D_w \tag{4d}$$

This is the mode for measuring loaded radial runout in which case X_h is the runout. Since it is dependent on the dynamic modulus, one may expect that the loaded radial runout measurement is more directly speed dependent than the radial force variation. Nevertheless, Equations (4c) and (4d) clearly represent the force variation and loaded runout measurements as being mechanistically related through the dynamic modulus of the tire/wheel assembly. At low speed (or frequency) the dynamic modulus is essentially equal to the radial spring rate of the tire. Hence, the low-speed radial force variations and loaded radial runout are related to each other by the radial stiffness of the tire [5].

Similarly, on analyzing the Norton System, we obtain:

$$F_t - F_h = 0 \tag{5a}$$

where

F_t = force produced by D_w

$= D_w(X_w - X_h)$

and X_w = dimensional runout in the tire/wheel assembly

Then

$$D_w(X_w - X_h) = F_h \tag{5b}$$

For $X_h = 0$, as in measurement of force variation, the observed force is:

$$F_h = D_w X_w \tag{5c}$$

And for measurement of loaded radial runout with $F_h = 0$, the observed runout variation is:

$$X_h = X_w \tag{5d}$$

Thus it is concluded that the loaded radial runout in a tire/wheel assembly is directly related to its radial force variation.

Note that, in general, if the resisting force, F_h, is obtained from a compliant spindle of modulus D_s, such that $F_h = D_s \cdot X_h$, we find that, on substituting for X_h in Equation (4b), the following relationship is obtained:

$$F_h = F_w \cdot \frac{D_s}{D_s + D_w} \tag{6}$$

Equation (6) indicates that the actual force at the interface of the wheel and spindle is not equal to the nonuniformity force, F_w. Rather, the

wheel/spindle force resulting from the excitation, F_w, may be significantly different in amplitude and phase angle in accordance with the dynamic properties of D_w and D_s in the combination defined in Equation (6). This equation then represents, in a general form, the way in which the tire/wheel assembly interacts dynamically with the system on which it is mounted. It characterizes the concept of "impedance coupling" which is treated in more detail in the following sections.

2.3 Test Machine Model

In order to measure tire/wheel nonuniformities, the assembly is mounted on a test machine with provision for the wheel to be rolled under load on a drum. The forces or displacements are then measured either at the spindle or in the drum. For this discussion, it is assumed that the wheel rolls against a rigid drum while mounted on a spindle instrumented to measure force, as is the case with the test machine being used in the MVMA-sponsored research. In order to measure force, some deflection of the spindle must be allowed, in which case dynamic response in the frequency range of measurements may, and indeed does, occur with the test machine.

Any dynamic system with an input and output connection, such as the transducer on the test machine, can be represented by an equivalent "T" or "π" system [1]. Figure 4 shows a "π" system representation of the transducer. On the left is the input which is the spindle/hub connection point. The force F_h may be envisioned as the radial-direction force coming from the tire/wheel assembly, while F_c is the force imposed on the carriage in the same direction. D_1 and D_3 are not physically connected to ground, but in the π network representation of the system, may be envisioned as masses connected to inertial ground. At the right-hand side is the connection to the machine loading carriage. The modulus, D_2, is nominally the stiffness of the transducer flexure, while D_1 and D_3 may be visualized as the inertial stiffnesses arising from the masses on each end of the transducer.

The transducer is mounted to a movable carriage which is hydraulically actuated to load the wheel against the drum. The carriage mounting point is not infinitely stiff, hence it may also contribute to the dynamics of the system through its mass, stiffness, and damping properties. The

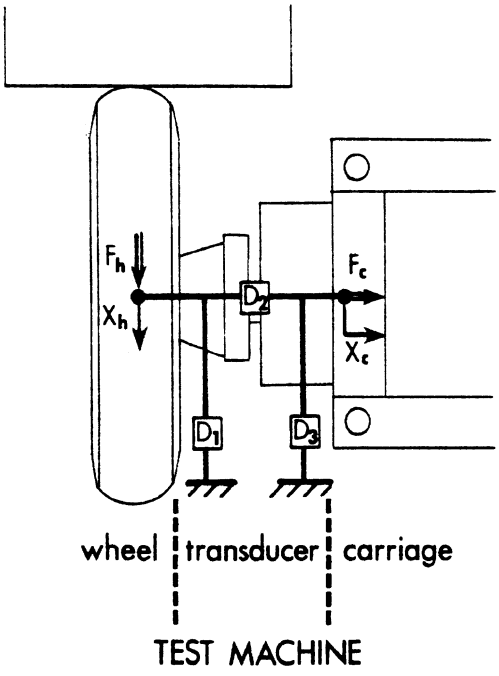

Figure 4. A "π" system representation of the transducer on the MTS Tire Test Machine.

carriage can be represented by a modulus, D_c, such that the model for the total tire/wheel, transducer, and machine system is that shown in Figure 5. It is assumed that, except as represented here, the remainder of the test machine is infinitely stiff (e.g., per the drum stiffness values included in the UMTRI machine specification [6]) and does not contain any excitation sources correlated to the tire/wheel excitation.

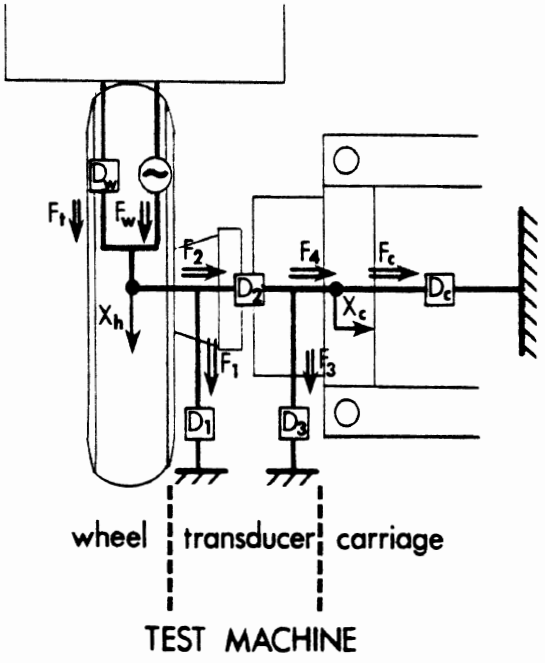

Figure 5. Dynamic model for the tire/wheel assembly, force transducer, and the test machine.

3. TIRE TEST MACHINE DYNAMIC EFFECTS

A dynamic model of a tire/wheel/test machine system, as assembled in Section 2, can now be used to explain the nature of dynamic interactions that occur in the measurement process. The governing equations can be written by simply summing forces at the connecting nodes for the model shown in Figure 5:

At the spindle,

$$F_w + F_t - F_2 - F_1 = 0 \tag{7a}$$

At the transducer-carriage interface,

$$F_4 - F_3 - F_c = 0 \tag{8a}$$

Now the forces associated with each modulus are equal to the modulus times the differential motion across each. Thus Equations (7a) and (8a) can be written as

$$F_w + D_w(0-X_h) - D_2(X_h-X_c) - D_1(X_h-0) = 0 \tag{7b}$$

$$D_2(X_h-X_c) - D_3(X_c-0) - D_c(X_c-0) = 0 \tag{8b}$$

Equation (8b) can be solved for X_c, the motion of the carriage, viz.:

$$X_c = \frac{D_2}{D_2 + D_3 + D_c} X_h \tag{8c}$$

and on substituting for X_c in Equation (7b), the following result is obtained for F_w:

$$F_w = \left[(D_w+D_1) + \frac{D_2(D_3 + D_c)}{D_2 + D_3 + D_c}\right] X_h \tag{7c}$$

Since we are not really interested in separating the dynamic effects of D_3 and D_c, they can be lumped together as a machine modulus, D_m, i.e.,

$$D_m = D_3 + D_c$$

Equation (7c) becomes

$$F_w = \left[D_w + D_1 + \frac{D_2 D_m}{D_2 + D_m}\right] X_h \qquad (7d)$$

Though we now have the governing equation, the interest at this point is not in the motion of the spindle, X_h, but rather in the measurement of F_w. Thus far, the force measured by the test machine, F_m, does not show up in the equation. It can only be obtained by defining how it is measured, which in turn is dependent on the method by which the transducer is calibrated.

3.1 Calibration

The force measurement in the test machine is obtained by means of strain gauge measurements of deflections in the transducer flexures. In terms of the model shown in Figure 5, F_m is proportional to $(X_h - X_c)$, that is

$$F_m = C(X_h - X_c) \qquad (9)$$

where C is the calibration factor which is a constant for a static calibration, or a function of frequency in the case of dynamic calibration.

Conceptually, calibration is achieved by imposing a known force (a calibration force, F_{cal}) in place of the tire/wheel assembly to establish the correct scale for the measured value, F_m. The calibration process is represented in the model by substituting a calibration force, F_{cal}, for the wheel excitation force, F_w. Combining Equations (7d), (8c), and (9) to eliminate X_h and X_c:

$$F_w = F_{cal} = \left[D_w + D_1 + \frac{D_2 D_m}{D_2 + D_m}\right]\left[\frac{D_2 + D_m}{D_m}\right] F_m/C \qquad (10)$$

The calibration is then simply the determination of a value for C such that $F_m = F_{cal}$. The correct calibration factor is obviously:

$$C = \left[D_w + D_1 + \frac{D_2 D_m}{D_2 + D_m}\right]\left[\frac{D_2 + D_m}{D_m}\right] \qquad (11)$$

The bracketed terms are complex quantities whose amplitude and phase are frequency dependent, thus illustrating the need for dynamic calibration. However, a true dynamic calibration is not possible. Thus the various alternative calibration methods are analyzed below to identify their error sources.

a) Static Calibration. The wheel is removed (D_w=0) and a reference load cell is used to impose F_{cal} statically. Thence, each modulus has its zero frequency value (indicated by a "o" subscript), and Equation (10) takes the form:

$$F_{cal} = \left[D_{1o} + \frac{D_{2o} D_{mo}}{D_{2o} + D_{mo}}\right]\left[\frac{D_{2o} + D_{mo}}{D_{mo}}\right] F_m/C \qquad (12)$$

Setting $F_m = F_{cal}$ in the calibration yields:

$$C = \left[D_{1o} + \frac{D_{2o} D_{mo}}{D_{2o} + D_{mo}}\right]\left[\frac{D_{2o} + D_{mo}}{D_{mo}}\right] = \text{Constant} \qquad (13)$$

Substituting this value for "C" back into Equation (10) then yields the expression for the force measured by the test machine:

$$F_m = F_w \cdot \frac{\left[D_{1o} + \frac{D_{2o} D_{mo}}{D_{2o} + D_{mo}}\right]\left[\frac{D_{2o} + D_{mo}}{D_{mo}}\right]}{\left[D_w + D_1 + \frac{D_2 D_m}{D_2 + D_m}\right]\left[\frac{D_2 + D_m}{D_m}\right]} \qquad (14)$$

From this equation, it is clear that, in general, the measured force will not be equal to the nonuniformity force within the tire/wheel assembly for several reasons:

1) The calibration factor is a real constant, whereas the dynamics represented by the denominator vary in amplitude and phase angle with frequency.

2) The presence of the wheel modulus in the denominator tends to attenuate the measured force even at zero frequency. Its effect can be estimated for the radial force direction at zero frequency by making the assumptions

D_w = tire spring rate = K_w

D_1 = transducer mass property $\cong$ 0

D_m = machine static stiffness >> D_2

D_2 = transducer flexural stiffness

Then

$$F_m = F_w \cdot \frac{D_2}{K_w + D_2} \tag{15}$$

From this equation it is evident that, if the transducer stiffness is only an order of magnitude greater than the tire spring rate (i.e., $D_2 = 10 \cdot K_w$), the measured force will have approximately a 10% error. In practical terms, Equation (15) would indicate that for measurements on dual tire assemblies, which have a nominal stiffness of 10,000 lb/in, the transducer stiffness must be at least 1,000,000 lb/in for errors no greater than 1%. (This error analysis was the basis for the test machine stiffness specifications developed by this Institute [6].)

As an alternative, one might suggest a static calibration process in which the wheel is left in place and loaded against the drum to add the stiffness, D_{wo}, to the calibration factor obtained. Aside from the complication that the static calibration equipment would have to be redesigned to accommodate this procedure, only an approximate correction is obtained because the static tire spring rate differs from its value when rolling.

With a static calibration applied, the numerator of Equation (14) is simply a constant and the measured force will be equal to the wheel excitation force, F_w, times a complex function representing the response of the system. That complex function may be considered a response function having a gain and phase influence dependent on temporal frequency. An example of the response function gain for the radial direction of a dual wheel assembly on the MTS Test Machine is shown in Figure 6a. The gain is measured as the transfer function between the input of a hydraulic exciter applied to the wheel in the radial force direction and the machine-measured radial force output. The response function shows regions of high gain associated with modal resonances of the system. The lowest peak at about 35 Hz is a resonance associated with the wheel mass and the radial stiffness of the transducer. The higher frequency resonances represent more complex modes. The effect of these resonances is to cause the transducer measurement gain to vary with frequency. Figure 6b illustrates the effect on the measured amplitude of radial force variations in a wheel assembly by a spectral map of the amplitude as the wheel is run at different speeds. As evident on the map, the measured forces reflect the system resonances by increases in amplitude at speeds where they individually tune to the resonant modes.

b) Dynamic Calibration. In order to correct for the influence of dynamic behavior on the measured force as shown above, a dynamic calibration may be considered. The process is similar to static calibration except that the calibration input force is swept through frequency and C is measured as a function of frequency, ω. The calibration factor, C, then has frequency-dependent amplitude and phase properties. In its generalized form:

$$C = \left[D_w + D_1 + \frac{D_2 D_m}{D_2 + D_m}\right]\left[\frac{D_2 + D_m}{D_m}\right] = f(\omega) \qquad (16)$$

The value of D_w depends on whether the wheel is present during the calibration and whether it is loaded against the drum. In effect, the dynamic measurement of C is part of what is often called "dynamic characterization." When applied as a correction to the measured force, it is called "dynamic compensation." In this case, the describing equation takes the form

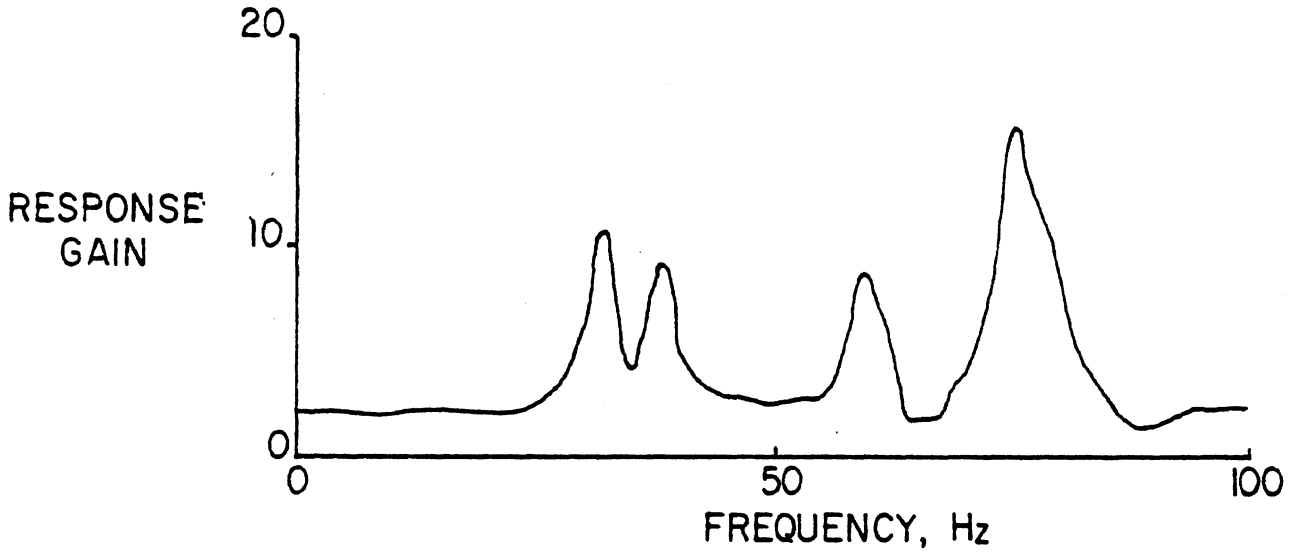

Figure 6a. Plot of Radial Response Function Bias

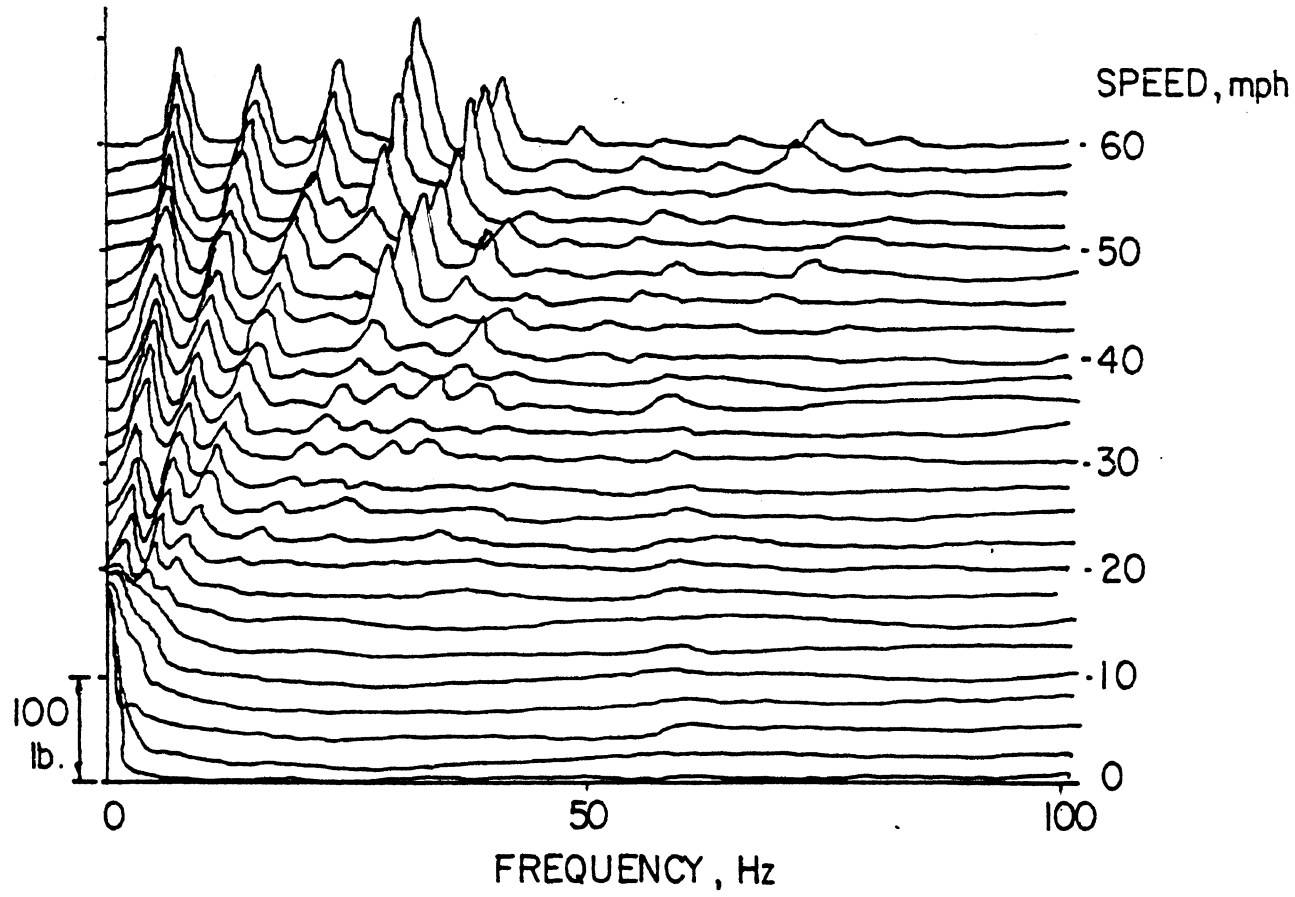

Figure 6b. Spectral Map of Radial Force

Figure 6. Effect of tire test machine dynamics on force measurements.

shown below, where the subscript "C" denotes the dynamic modulus present in the calibration process, i.e.,

$$F_m = F_w \frac{\left[D_{wC} + D_{1C} + \frac{D_{2C}D_{mC}}{D_{2C} + D_{mC}}\right]\left[\frac{D_{2C} + D_{mC}}{D_{mC}}\right]}{\left[D_w + D_1 + \frac{D_2 D_m}{D_2 + D_m}\right]\left[\frac{D_2 + D_m}{D_m}\right]} \tag{17}$$

Now, Equation (17) would indicate valid force measurements if the dynamic properties during testing are identical to those during calibration. To achieve this, the wheel must be mounted during calibration, and ideally, even rolling to exhibit the proper stiffness properties. In that case, the wheel is imposing its own excitation, F_w, during the calibration process; although theoretically it can be separated out because it is uncorrelated with the calibration signal.

Applied in this manner, the dynamic calibration does eliminate machine and tire dynamic effects from the measured force (although, unintentionally, also including tire modal resonances). However, a test of this approach on the machine has revealed two major shortcomings to its practical implementation. One, the dynamic characterization process tends to be quite lengthy and time-consuming. Second, the dynamic behavior is quite sensitive to the operating conditions—specifically, the tire, inflation pressure, load, carriage position, and other lesser variables. In particular, the resonances have a high amplitude and narrow bandwidth, making it difficult to compensate accurately. Figure 7 illustrates the problem, showing the response in the radial (z), lateral (y), and tractive (x) directions under radial excitation. When correcting for amplitude ratios on the order of 10:1 or 20:1, good accuracy is difficult to achieve because a shift in the resonant frequency of only 1-2 Hz causes large errors. At best, the technique is only reasonable at frequencies far from the resonances, which in this case limits the usable range to 20 Hz and below.

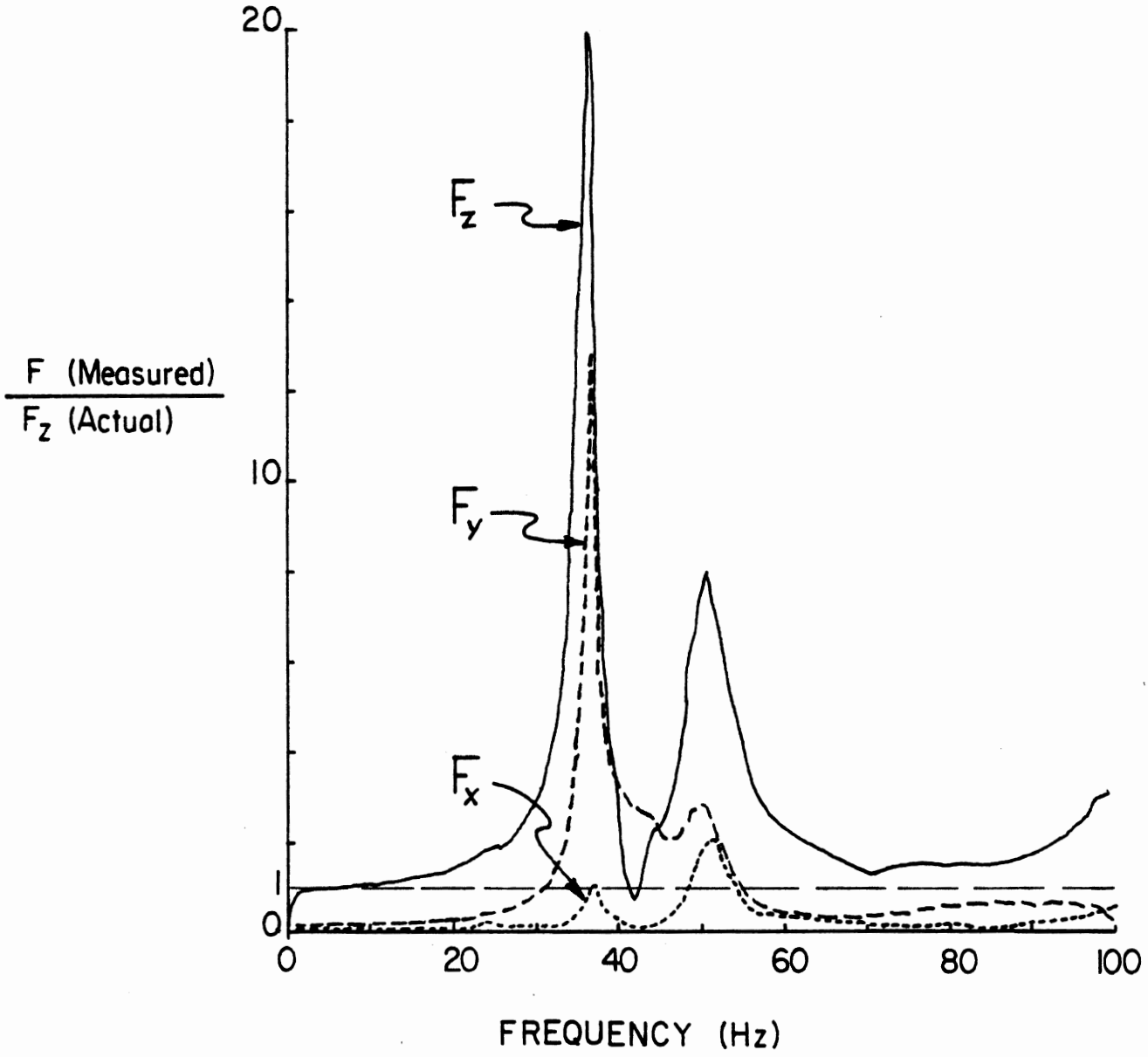

Figure 7. Forces measured in the radial (F_z), lateral (F_y), and tractive (F_x) force directions on the test machine with radial excitation only.

3.2 Cross-Axis Dynamics

The full story of machine dynamic interaction is not entirely represented by the dynamic effects on the individual axes as reflected in Figure 6, but also involves cross-coupling between axes, as evident in Figure 7. Because transducer manufacturers are not able to construct load transducers that respond purely to the individual axes, the measurement on each axis includes some interaction from the other axes (whether instrumented for measurement or not) known as cross-talk. On the other hand, the presence of compliance within the transducer or machine will allow mechanical cross-coupling of forces between axes through the tire/wheel assembly under test by means that will be discussed later. Cross-coupling within the wheel assembly itself is to be expected and is one of the quantities to be measured as a part of the nonuniformity effect. However, with a compliant transducer exhibiting mechanical interaction between axes, additional cross-coupling phenomena will occur and add to the measurement errors.

To understand these effects systematically, a generalized cross-coupling model is shown in Figure 8 for the x translation axis. The system has five degrees of freedom—three translation and two rotation. (The spin axis rotation, θ_y, is decoupled from the transducer by the wheel bearings and is hence neglected.)

In the figure, cross-axis dynamics are represented via two mechanisms. First, displacements along one axis induce a force along another through inertial or tire flexural reactions. These are mechanical cross-coupling effects. On the test machine, for example, a radial force bends the cantilevered transducer so as to cause an overturning rotation, θ_x. The lateral movement at the tire contact patch then generates a lateral force. Hence, F_z and F_y forces are closely coupled and the presence of one in the tire/wheel assembly results in the measurement of both on the test machine. This phenomenon is appropriately called dynamic cross-coupling and is reflected in the model by the cross-coupling moduli D_{xy}, D_{xz}, etc. Secondly, due to the imperfections in fabrication of the transducer, loads imposed along one axis will ficticiously register on other axes (i.e., transducer cross-talk). Inasmuch as the source of the cross-talk signal

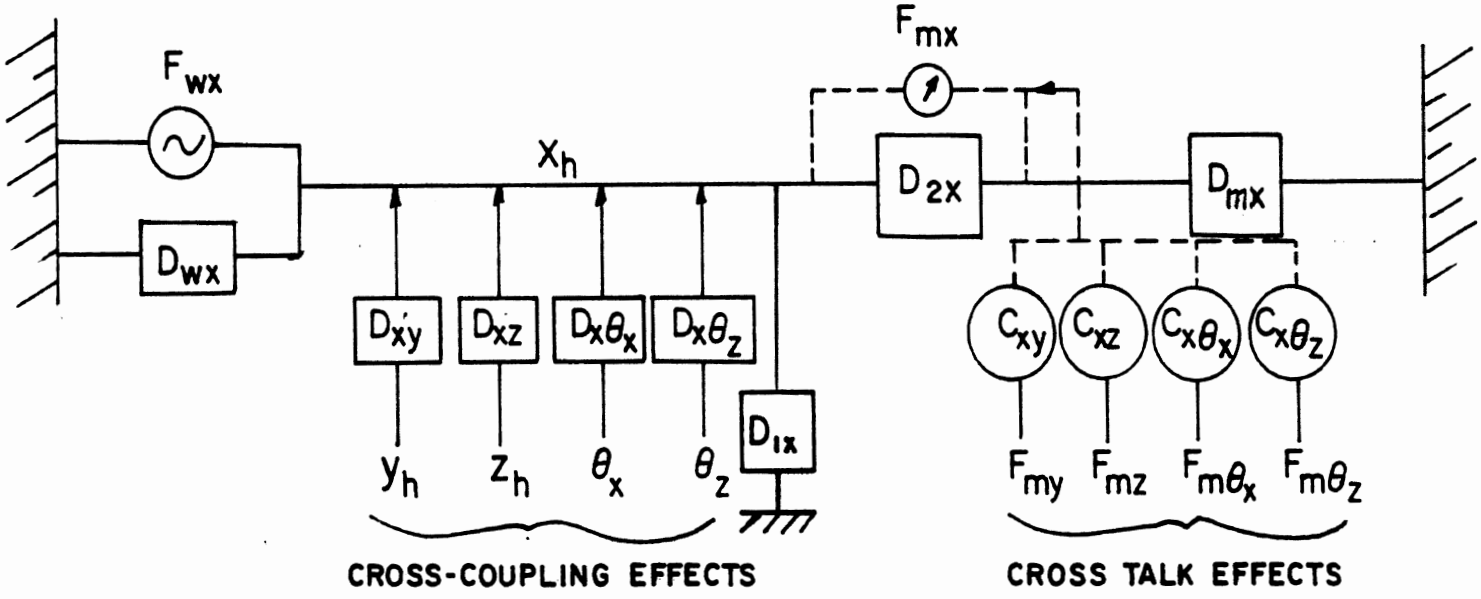

Figure 8. Dynamic model of the tire/wheel assembly and test machine for the x-axis with cross-coupling and cross-talk effects.

is strain in the flexures of the loaded axis, the magnitude of the cross-talk signal derived from the loaded axis should always be proportional to the primary signal on that axis. Hence, cross-talk is not a direct manifestation of machine dynamic interactions, but simply an error in the ability to correctly resolve the force axes into the desired orthogonal system. The cross-talk effects themselves have no dynamic behavior below the resonant frequencies of the flexures. Hence, the application of static cross-talk compensation properly corrects for the cross-talk interactions represented by the dashed lines and C_{xy}, C_{xz}, etc., coefficients shown in the figure.

The proof that cross-talk is independent of dynamics is difficult to demonstrate on a transducer with mechanical cross-coupling, for tests of just the transducer alone will always manifest some mechanical cross-coupling through the mass of the fixtures through which the load is applied.

The cross-coupling effects deriving from the cross-coupling moduli in Figure 8 are dependent on the absolute displacements on each axis at the wheel spindle location. Rederiving the governing equations equivalent to the earlier Equations (7) and (8) for the cross-coupling model in Figure 8 leads to results of the following form:

$$F_{wx} = [D_x+D_{xy}+D_{xz}+D_{x\theta z}+D_{x\theta x}] \cdot x_h - D_{xy}y_h - D_{xz}z_h - D_{x\theta x}\theta_x - D_{x\theta z}\theta_z \quad (18a)$$

$$F_{wy} = -D_{xy}x_h + [D_y+D_{xy}+D_{yz}+D_{y\theta z}+D_{y\theta x}]y_h - D_{yz}z_h - D_{y\theta x}\theta_x - D_{y\theta z}\theta_z \quad (18b)$$

$$F_{wz} = -D_{xz}x_h - D_{yz}y_h + [D_z+D_{xz}+D_{yz}+D_{z\theta z}+D_{z\theta x}]z_h - D_{z\theta x}\theta_x - D_{z\theta z}\theta_z \quad (18c)$$

$$F_{w\theta x} = -D_{x\theta x}x_h - D_{y\theta x}y_h - D_{z\theta x}z_h + [D_{\theta x}+D_{x\theta x}+D_{y\theta x}+D_{z\theta x}+D_{\theta z\theta x}]\theta_x - D_{\theta z\theta x}\theta_z \quad (18d)$$

$$F_{w\theta z} = -D_{x\theta z}x_h - D_{y\theta z}y_h - D_{z\theta z}z_h - D_{\theta z\theta x}\theta_x + [D_{\theta z}+D_{x\theta z}+D_{y\theta z} + D_{z\theta z}+D_{\theta x\theta z}]\theta_z \quad (18e)$$

where a modulus with a single subscript (of the form D_i) is the dynamic coefficient for axis "i" (i=x,y,z, θx or θz) and

$$D_i = \left[D_{wi} + D_{1i} + \frac{D_{2i} \cdot D_{mi}}{D_{2i} + D_{mi}}\right] \quad (19)$$

A modulus with a double subscript (the form D_{ij}) is the cross-coupling dynamic modulus for axis "j" on "i." Also in the above equations:

x_h, y_h, z_h = hub translational deflections

θx, θz = hub rotational deflections

The above equations relate the forces on each axis to the deflections on all axes. From Equations (8c) and (9) it can be shown that the deflection along each axis is related to the force measured on the axis by an equation of the form shown below for the x-direction.

$$x_h = F_{mx} \cdot \frac{1}{C_x} \cdot \frac{D_{2x} + D_{mx}}{D_{mx}} \quad (20)$$

The Equations (18) can then be reduced to a relationship between forces, i.e.:

$$F_{wx} = \alpha_x F_{mx} + \alpha_{xy} F_{my} + \alpha_{xz} F_{mz} + \alpha_{x\theta x} F_{m\theta x} + \alpha_{x\theta z} F_{m\theta z} \quad (21a)$$

$$F_{wy} = \alpha_{xy} F_{mx} + \alpha_y F_{my} + \alpha_{yz} F_{mz} + \alpha_{y\theta x} F_{m\theta x} + \alpha_{y\theta z} F_{m\theta z} \quad (21b)$$

$$F_{wz} = \alpha_{xz} F_{mx} + \alpha_{yz} F_{my} + \alpha_z F_{mz} + \alpha_{z\theta x} F_{m\theta x} + \alpha_{z\theta z} F_{m\theta z} \quad (21c)$$

$$F_{w\theta x} = \alpha_{x\theta x} F_{mx} + \alpha_{y\theta x} F_{my} + \alpha_{z\theta x} F_{mz} + \alpha_{\theta x} F_{m\theta x} + \alpha_{\theta x\theta z} F_{m\theta z} \quad (21d)$$

$$F_{w\theta z} = \alpha_{x\theta z} F_{mx} + \alpha_{y\theta z} F_{my} + \alpha_{z\theta z} F_{mz} + \alpha_{\theta x\theta z} F_{m\theta x} + \alpha_{\theta z} F_{m\theta z} \quad (21e)$$

Note that a symmetric matrix is evident in the equational relationships. The coefficients on the main diagonal are obtained from substitution of Equations (19) and (20) into Equation (18) and have the form as shown here for the x-direction:

$$\alpha_x = \left[D_{wx} + D_{1x} + \frac{D_{2x} D_{mx}}{D_{2x} + D_{mx}} + D_{xy} + D_{xz} + D_{x\theta x} + D_{x\theta z} \right] \cdot \frac{1}{C_x} \cdot \frac{D_{2x} + D_{mx}}{D_{mx}} \tag{22}$$

The expression for other coefficients on the main diagonal can be obtained from Equation (22) by substituting other direction indices for the subscript "x". It may be recognized that the diagonal coefficients reflect the relationship between the applied and measured forces on a given axis as influenced by vibrations on that axis (the first three terms in the brackets), as well as additional forces imposed on the primary axis as a result of the constraint of its motion by mechanical cross-coupling to the other axes.

The off-diagonal coefficients represent the influence of cross-coupled motions on the alternate axes, and have the form:

$$\alpha_{ij} = - D_{ij} \cdot \frac{1}{C_j} \cdot \frac{D_{mj}}{D_{2j} + D_{mj}} \tag{23}$$

where

i is the primary axis, and

j is the alternate axis

The off-diagonal coefficients reflect the forces imposed on a primary axis due to motions on the other axes, and provide the path for dynamic resonances on one axis to appear on others.

Reduced to this form, it is now possible to evaluate the complexity of compensation for cross-coupling effects. Mathematically, the process is one of evaluating the 15 coefficients for Equations (21a-e) and then operating on the measured data to yield corrected estimates for the wheel force quantities. (Note that in practice, F_w is the input and F_m is the

output, so that a matrix inversion operation is required to obtain the coefficients for Equation (21).) The main diagonal coefficients, as given in Equation (22), represent the dynamic characterization for each axis. In this case, the dynamic behavior is further modified by the cross-coupling moduli reflecting inertial properties of the wheel as well as the cross-coupling stiffness derived from its contact with the drum. Gyroscopic effects and tire relaxation length effects therefore become involved, suggesting that speed assumes first-order significance in the cross-coupling dynamics.

The off-diagonal terms essentially represent forces imposed on the primary axis as the result of deflections on the alternate axes. Their magnitude depends on both the cross-coupling moduli and the amplitude of deflections on the other axes. These terms account for the obvious cross-coupling of resonances to other measurement axes. As was seen in Figure 7, excitation in the z-direction reveals a sharp resonance at approximately 37 Hz. Because this resonance involves rotation in the overturning moment direction, the tire attempts to move laterally at the contact patch. When in contact with the drum, an F_y force is generated and measured, as was evident in the figure. When the tire is moved away from the drum, the F_y response effectively disappears, leaving only the residual component associated with inertial cross-coupling effects.

The experimental procedure for measuring the dynamic cross-coupling effects necessary for comparison involves two steps. One is the dynamic characterization along each axis equivalent to determining the coefficients on the main diagonal (Eq. (22)). In effect, this relates the measured force to an input force on that axis in the presence of dynamic effects of the machine/tire combination along that axis. In contrast to the dynamic calibration explained in the preceding section, however, the characterization now includes tire stiffness effects on the primary axis derived from cross-coupled motions on the other axes. The total of these effects is what would actually be measured in an attempt to dynamically characterize a particular axis.

The second step involves characterization of the cross-coupling of each axis to the primary axis—the off-diagonal terms in Equation (21).

The characterization represents the transfer functions for the force induced on the primary axis by deflections on each of the other axes. While this would imply measurement of the deflections on all axes, those measurements are not necessary but can be deduced from the force measurements on the alternate axes obtained from the transducer using the relationship given in Equation (20).

As with the single-axis dynamic calibration described in the previous section, a valid compensation for cross-axis dynamics necessitates characterization at actual operating conditions. In addition to the recognized sensitivity to individual tires, inflation pressure, load, and carriage position, a first-order sensitivity to speed is expected as well. Finally, to accomplish the compensation, all degrees of freedom must be instrumented and employed. Instrumentation on the overturning moment axis is absent on the Model 860 test machine thus precluding the implementation of this process.

3.3 Summary of Machine Dynamic Interactions

In summary, it is seen that the measurement of the force variations in a tire/wheel assembly using a compliant test machine has the potential for three types of errors.

1) Static Force Attenuation - At the level of simply trying to measure forces at very low speeds, the compliance of the machine will attenuate the force variations produced by the tire/wheel assembly. The effect is described by Equation (15) when the primary compliance is in the transducer:

$$F_m = F_w \cdot \frac{D_2}{K_w + D_2} \tag{15}$$

where

D_2 = transducer flexural stiffness

K_w = tire spring rate

For a very stiff machine:

$$D_2 >> K_w$$

$$F_m \simeq F_w$$

For a very compliant machine:

$$K_w >> D_2$$

$$F_m \simeq 0$$

The above equations simply reflect the fact that the force variation observed is proportional to the stiffness of the machine on which the measurement is obtained, and for negligible error the machine must be nominally 100 times stiffer than the tire/wheel being measured.

2) Dynamic Resonances - In the case of high-speed testing in which harmonic excitations in the tire/wheel assembly approach the resonant frequencies of the system, the forces imposed and measured on the spindle may be greatly exaggerated over the actual excitation produced by the nonuniformity. The behavior is described by Equation (14), which can be reduced to the form:

$$F_m = F_w \cdot \frac{C}{[D_w + D_{m1}][D_{m2}]} \tag{24}$$

where

C = calibration factor

$$D_{m1} = D_1 + \frac{D_2 D_m}{D_2 + D_m}$$

$$D_{m2} = \frac{D_2 + D_m}{D_m}$$

Thus, the measured force will differ from that actually present in the wheel in accordance with the amplitude and phase properties of the overall dynamic system comprised of the wheel and the machine. The error will vary

with frequency as was shown in Figure 6. By the nature of their combination (in the denominator term), the dynamic influences of the tire/wheel assembly and the machine cannot be separated. The effects can only be eliminated by dynamic calibrations, in which process the dynamic behavior is measured and applied as the calibration factor. Because of the variations in the dynamics with the test conditions (wheel load, speed, and inflation pressure), the corrections must be determined for each test condition.

3) Dynamic Cross-Coupling - When the compliance properties of a test machine permit mechanical cross-coupling between axes, interaction of forces will occur. As characterized in Equations (18) - (23), the effects are dependent on:

- -the dynamic resonances in each direction (including all degrees of freedom)
- -the cross-axis deflection properties of the machine
- -the stiffness properties of the tire/wheel assembly.

The consequence is cross-axis excitatation of forces (i.e., force variations present along one axis will excite forces along other axes, as shown in Figure 7). Corrections for these effects require measurement of both the cross-coupling properties between all axes and the dynamic behavior on each axis. Because of the variations in the dynamics with the test condition, corrections must be determined for each condition, and in this case, will be particularly sensitive to the test speed.

4. DYNAMIC INTERACTIONS ON A VEHICLE

The ultimate need for developing a systematic treatment of dynamics in the preceding chapter is to understand the interactions of the tire/wheel assembly with a vehicle. It is well recognized that the high-speed force variations measured on a tire test machine are not equivalent to the force variations produced on the axle of a vehicle. In this chapter, an analysis of the wheel/vehicle system will be performed to clarify the mechanisms involved. Both analytical and experimental data will be used to illustrate the results. Though these data are inadequate to fully quantify the phenomena of interest, they identify certain difficulties that must be accommodated in the design of a method for experimentally measuring vehicle sensitivity to tire/wheel excitation.

4.1 Linear Model

A wheel mounted on the axle of a vehicle is analytically similar to the wheel/machine models described in the previous chapter. To illustrate the interaction between a wheel and the vehicle, consider the dynamic model shown in Figure 9. The vehicle from the axle up is represented by a "π" model. F_h and X_h, respectively, represent the force and motion at the hub of the wheel which is input to the axle or spindle of the vehicle. X_m represents motion of interest at another point on the vehicle, for example, at the driver's seat.

The nodal equations can be written for this model, and at the axle takes the form:

$$F_w - (D_w + D_u + D_s)X_h + D_s X_m = 0 \qquad (25)$$

At the nodal point defining X_m:

$$D_s X_h - D_s X_m - D_f X_m = 0 \qquad (26)$$

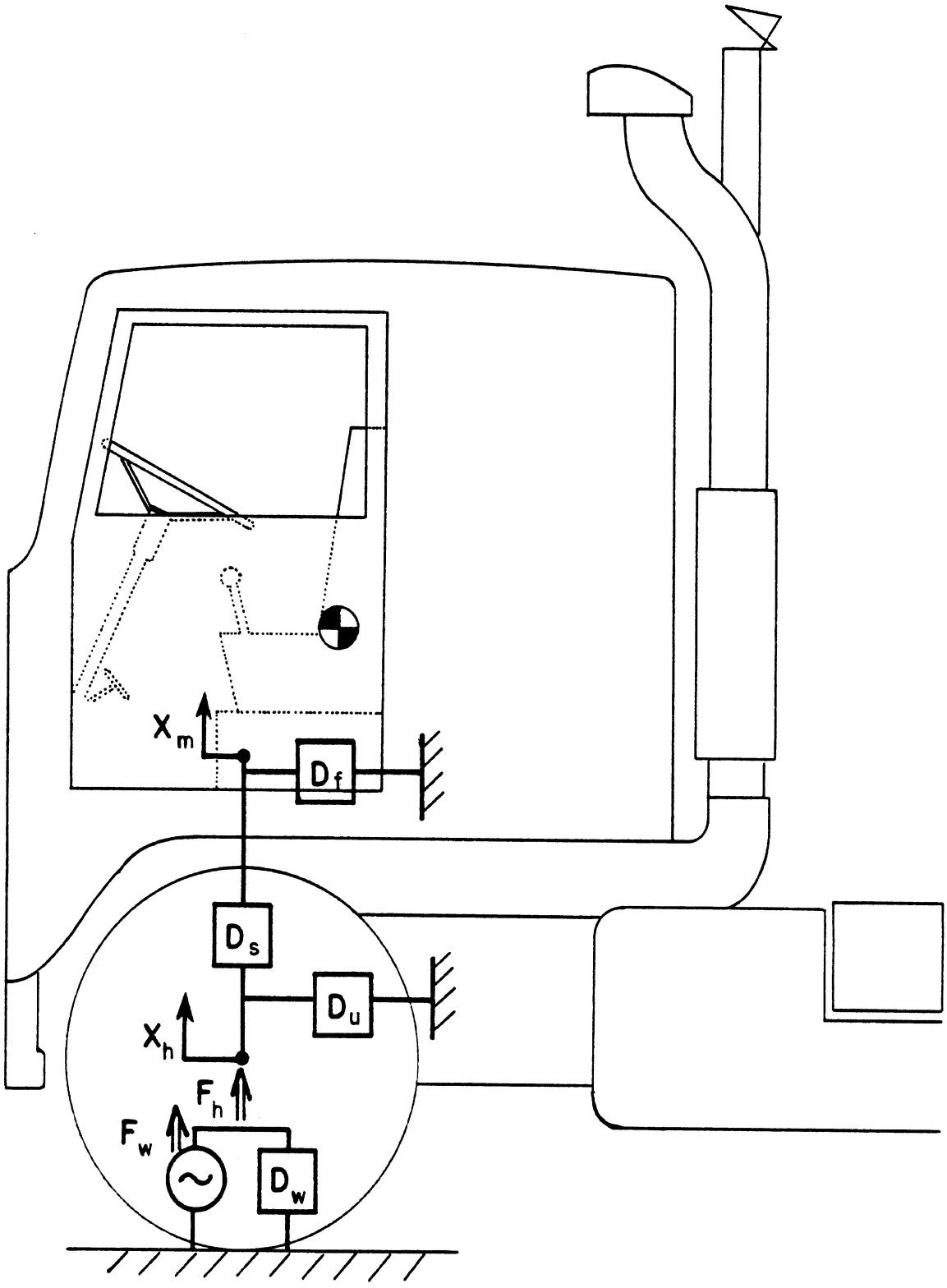

Figure 9. Dynamic model for a nonuniform tire/wheel assembly mounted on a truck.

The last equation relates motions of interest on the vehicle, X_m, to those at the hub, X_h. They are related by a transfer modulus, D_T, equivalent to a transmissibility function, i.e.,

$$X_m/X_h = \frac{D_s}{D_s + D_f} = D_T \tag{27}$$

It is equally of interest to consider the force/motion relationships at the hub inasmuch as it is the point of input for tire/wheel nonuniformity effects. The input force at the hub serving to excite the dynamic system is the nonuniformity force, F_w. Combining Equations (25) and (26) to eliminate X_m leads to the relationship:

$$F_w/X_h = D_w + D_u + \frac{D_s D_f}{D_s + D_f}$$

$$= D_w + D_A \tag{28}$$

where

D_w = driving point modulus of the tire/wheel assembly at its hub

D_A = driving point modulus at the axle or spindle of the vehicle.

Note that the force/motion relationship is determined by the algebraic summation of these two stiffnesses and is compatible with the notion that the stiffness observed at the hub of a vehicle is simply the total of the contributions from the tire/wheel assembly and from the vehicle.

Though described here as a modulus (stiffness), these properties of a vehicle are often characterized by the reciprocal variable, X_h/F_w, representing the motion response to force input. The variable is the receptance or compliance, and can be further related to motion at other points on the vehicle as follows:

$$X_h/F_w = \frac{1}{D_w + D_A} \tag{29}$$

$$X_m/F_w = \frac{X_h}{F_w} \cdot \frac{X_m}{X_h} = \frac{D_T}{D_w + D_A} \tag{30}$$

The quantity "X_m/F_w" may be considered as a transfer receptance or transfer compliance. Transfer inertance, relating accelerations on the vehicle, $\ddot{X}_m$, to the excitation force of the wheel, are only a transformation of the compliance function, i.e.,

$$\ddot{X}_m = -\omega^2 X_m$$

$$\therefore \ddot{X}_m/F_w = -\frac{\omega^2 D_T}{D_w + D_A} \tag{31}$$

Equations (27), (29), (30), and (31) describe all the properties of interest with respect to the vehicle and its response to tire/wheel nonuniformity excitation. Note that the vehicle behavior is characterized by three complex functions:

1) Transmissibility from the wheel hub to the sprung mass, D_T

2) The dynamic modulus of the wheel, D_w

3) The dynamic modulus of the axle or spindle, D_A

In practice, the number of variables required to fully characterize a vehicle are multiples of this number when multiple wheel positions, multiple vibration directions, and multiple points of interest on the vehicle (i.e., seating locations) are considered.

In characterizing the vehicle, it has not been necessary to include the force, F_h, which is the force variation experienced at the axle (i.e., the dynamic load imposed at the wheel bearings). It is critical to distinguish between the forces F_w and F_h because F_w is the force variation present in the tire/wheel assembly which serves to excite the dynamic system, whereas F_h is a force resulting from the dynamic behavior. The forces are not equivalent but are related by the equation:

$$F_h/F_w = \frac{D_A}{D_w + D_A} \tag{32}$$

The comparison of these forces will be illustrated in the next section for information purposes. However, the force on the axle, F_h, is of little utility, in general. Rather, in the interest of clarity in describing and communicating these dynamic phenomena, the analyst should think in terms of the excitation force, F_w, of interest as the measure of tire/wheel nonuniformity and the relevant input to the vehicle.

4.2 Examples of Wheel/Vehicle Dynamic Behavior

The general behavior of the dynamic system comprised of a nonuniform wheel on a vehicle can be quantified either by experimentally measuring the properties just described or by examining analytical models, such as the quarter-vehicle model shown in Figure 10. In the model, M is the sprung mass moving with displacement X_m of interest as the vibration input to the driver. The unsprung mass is separated into a component, M_a, representing the axle mass, and M_w, representing the wheel mass. Both move with displacement, X_h, with the force between them, F_h, equivalent to the vertical load carried by the wheel bearings.

The equations of motion can be solved for a sinusoidal force input at the wheel, F_w. Typical examples will be shown here for purposes of illustration, using model parameters representative of a well-damped motor vehicle (i.e., with a sprung mass natural frequency of 1.5 Hz, an unsprung mass natural frequency of 12 Hz, and a damping level that is approximately 35 percent of critical).

Consider first the magnitude ratio of the axle force to the nonuniformity excitation force (F_h/F_w from Eq. (32)) as shown in Figure 11. At zero frequency, the axle modulus is zero, hence so is the ratio. Physically, this corresponds to the fact that the axle load at zero frequency is its static value, and any attempt to vary the force at this point will produce an infinite displacement of the vehicle. Approaching 1 Hz, the force ratio rises due to resonance of the sprung mass. However, because the suspension stiffness is much less than that of the tire, much of the excitation force is absorbed by the tire and does not get through to the

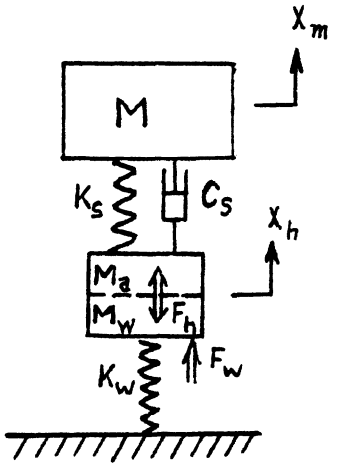

Figure 10. Quarter-vehicle model.

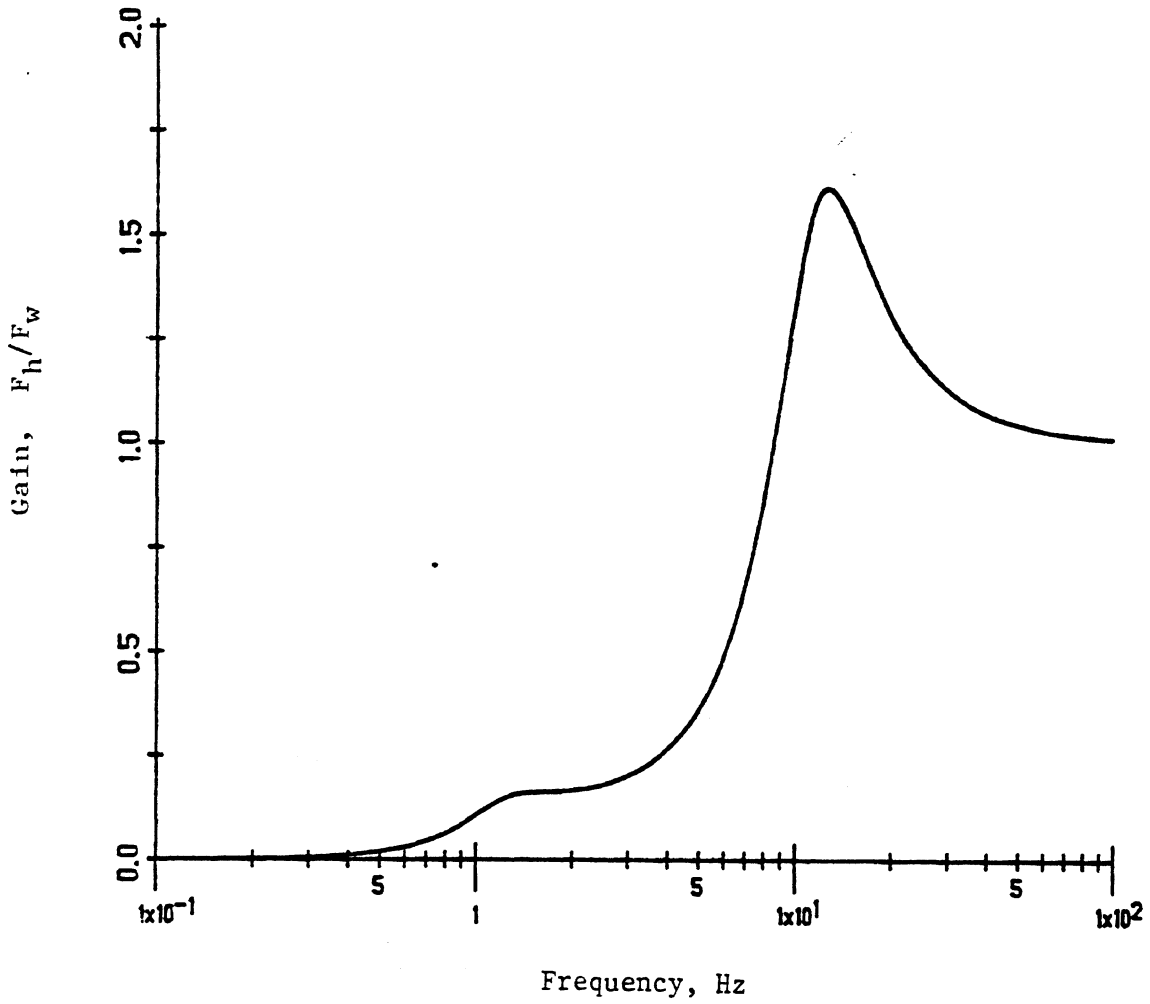

Figure 11. Plot of the ratio of axle force to nonuniformity excitation force for a quarter-vehicle model.

sprung mass. On the other hand, near the 12 Hz axle resonance, F_h becomes much greater than the excitation force because of the resonant motion of the axle. Thence, above axle resonance, the ratio diminishes to a value between zero and one, depending on whether most of the unsprung mass is in the wheel (M_w) or the axle (M_a). As pointed out in earlier discussions, the value of this plot is only informative for understanding the dynamics involved, but not germane to the analysis.

A better picture of the dynamics is seen in the motion response of the sprung and unsprung masses plotted in Figure 12a. At low frequency both move together at the amplitude determined by the force acting against the stiffness of the tire in contact with the ground. In such a plot, the low frequency asymptote is the tire compliance (the inverse of its stiffness). At higher frequencies, the motions of the sprung and unsprung masses differ in accordance with their resonances. Their difference is indicative of the suspension deflections, accounting for the shape of the axle force response seen in Figure 11.

From the standpoint of understanding the influence on ride vibrations, it is more meaningful to look at the acceleration response of the sprung mass in Figure 12b. Though the sprung and unsprung mass displacement magnitudes are approximately equal at their respective resonances, the acceleration experienced on the sprung mass is much greater at axle resonance due to its higher frequency. Thus, this figure would indicate that nonuniformity excitation from tire/wheel assemblies may potentially elicit the greatest vibration response when the nonuniformity frequency is near the axle resonant frequency.

Though simple analytical models provide a qualitative idea of the dynamic behavior to be expected, the quarter-vehicle model lacks representation of other important effects, namely, the multiple response modes that can occur in pitch or roll as well as bounce, and the suspension nonlinearity effects. Hence, experimental data is needed to establish credibility when dealing with a system as complex as a motor vehicle. Experimental data for comparison is not readily available, although several examples have been found. Figure 13 shows a plot of mobility* measurements taken at the front wheel of a European passenger car. The curves represent the mobility

*Mobility = 1/Impedance (see Section 2.1).

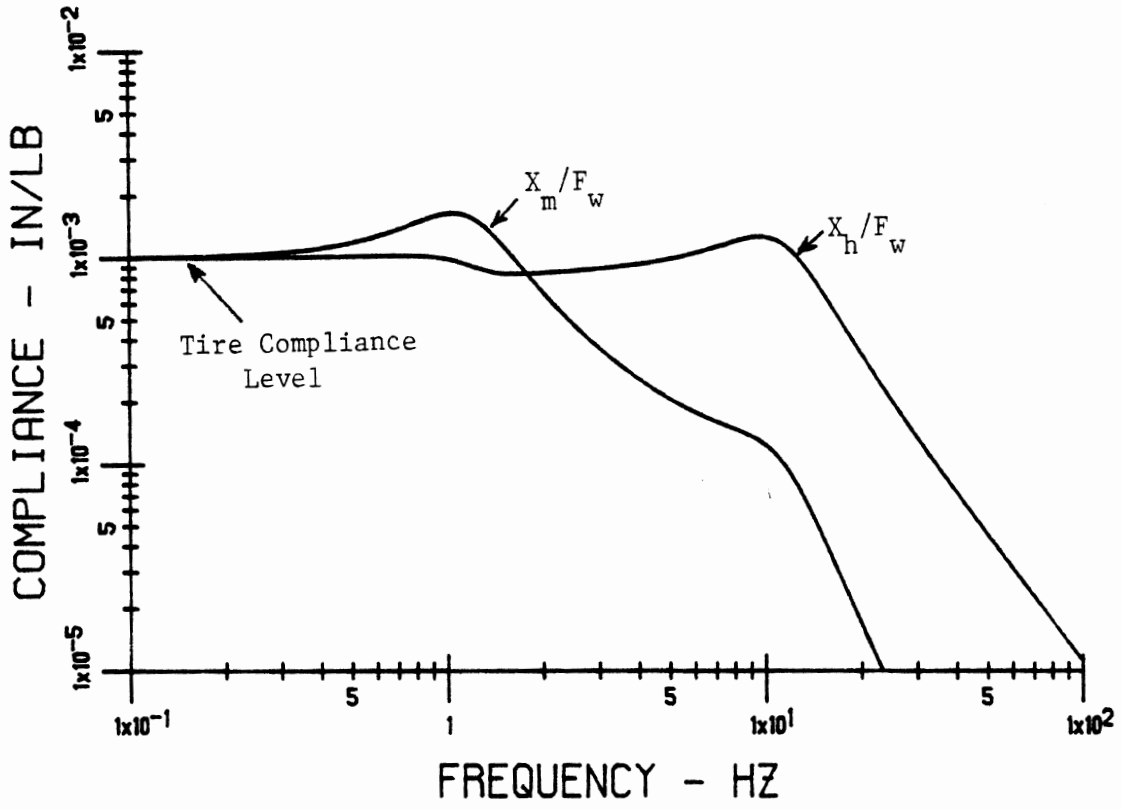

Figure 12a. Motions of the sprung and unsprung masses caused by nonuniformity excitation for a quarter-vehicle model.

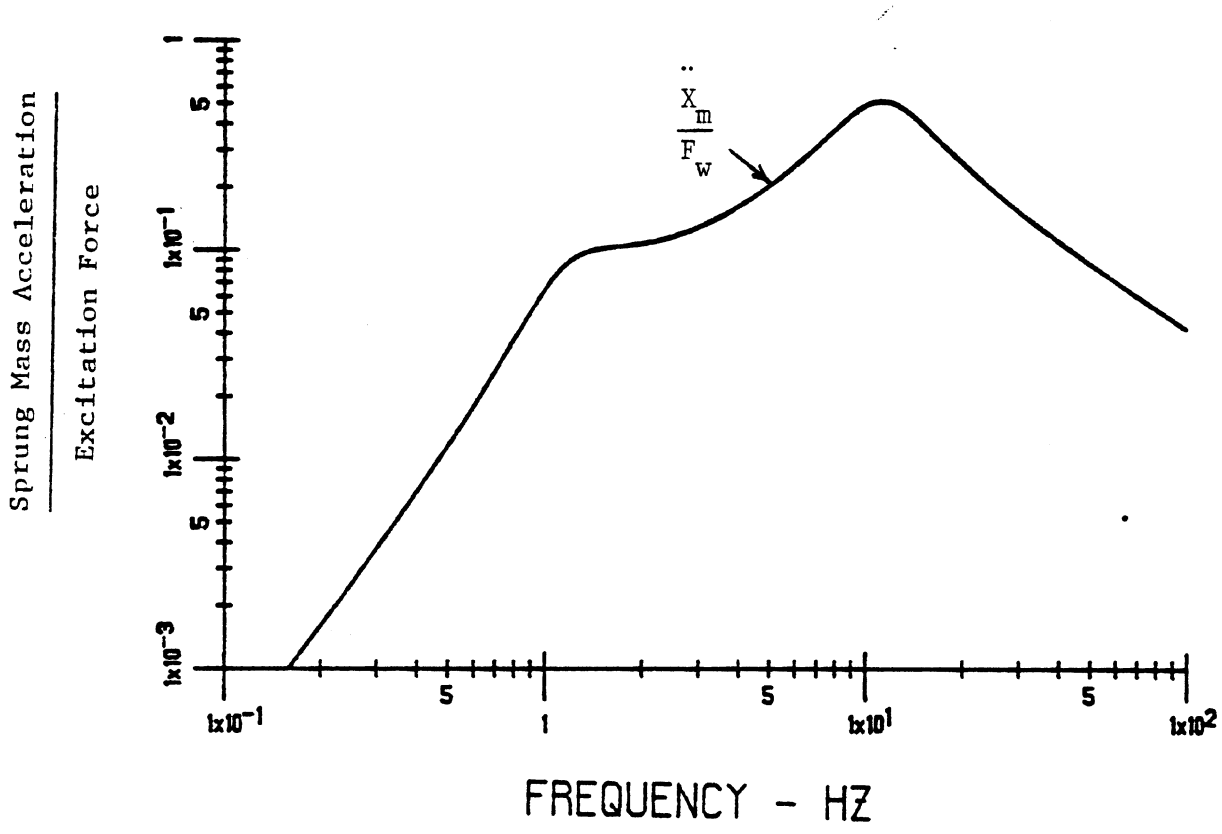

Figure 12b. Acceleration of the sprung mass casued by nonuniformity excitation for a quarter-vehicle model.

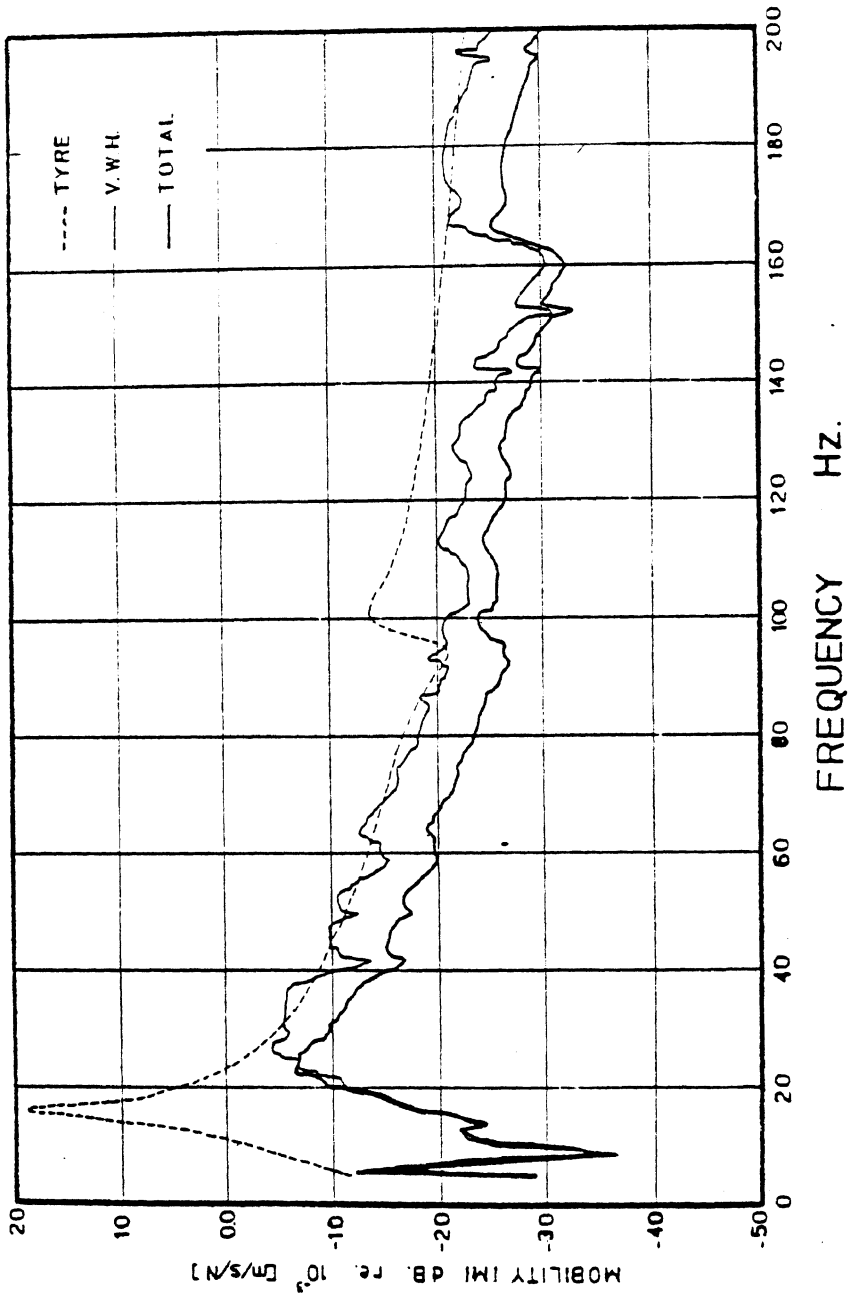

Figure 13. Mobility at the front-wheel hub on a passenger car [3].

of the tire and the vehicle wheel hub measured separately, and then the total for the combination. The mobility is $\dot{X}_h/F_w$, hence the curve for the "Total" is comparable to the plot of X_h/F_w (from Fig. 12a) multiplied by ω, the frequency. In Figure 13, a low-frequency resonance is evident at about 5 Hz which is most likely the sprung mass bounce resonance. Likewise, a second resonance is seen at just above 20 Hz which is most likely to be axle resonance. (Note: It appears that the frequency axis must be slightly in error in this figure because of the unusually high resonance frequencies indicated.) The relative magnitude of these two resonances agree reasonably well with that predicted from the linear quarter-vehicle model. Yet, the experimental curve shows more features, which may be expected when one considers that other resonances in pitch, roll, frame beaming, and additional modes will be present. Perhaps the most significant difference from the quarter-car model is that the attenuation above the axle resonance frequency is somewhat greater as measured on the vehicle in Figure 13.

A similar measurement on the front axle of a tractor is shown in Figure 14, using the driving point compliance as the measurement variable. This plot can be compared directly with that of X_h/F_w in Figure 12a. On the tractor, the compliance shows the sprung mass resonance at 1.5 Hz, along with axle resonance at about 12-15 Hz. Between these, other resonances occur due to the additional degrees of freedom associated with the pitch and bounce modes of the tractor and trailer, as well as the 3.2 Hz mode associated with "bounce on the tires" common to high friction leaf spring suspensions. Each of these peaks represents a vehicle sensitivity that can be excited by a tire/wheel nonuniformity. The amplitudes and frequencies at which these sensitivities occur will be specific to each vehicle, depending on properties associated with the suspension systems, loading, mass distribution, wheelbase, fifth wheel locations, and many other factors.

The accompanying vibration response in the cab is shown in Figure 15, both as displacement and acceleration response. Because ride vibrations are usually characterized by the acceleration spectrum, the acceleration response is the more meaningful of the two curves. The resonant behavior in the ranges of 3-5 Hz and 12-30 Hz indicate areas of greatest vehicle sensitivity to nonuniformity input. Though the high frequency peaks would appear to

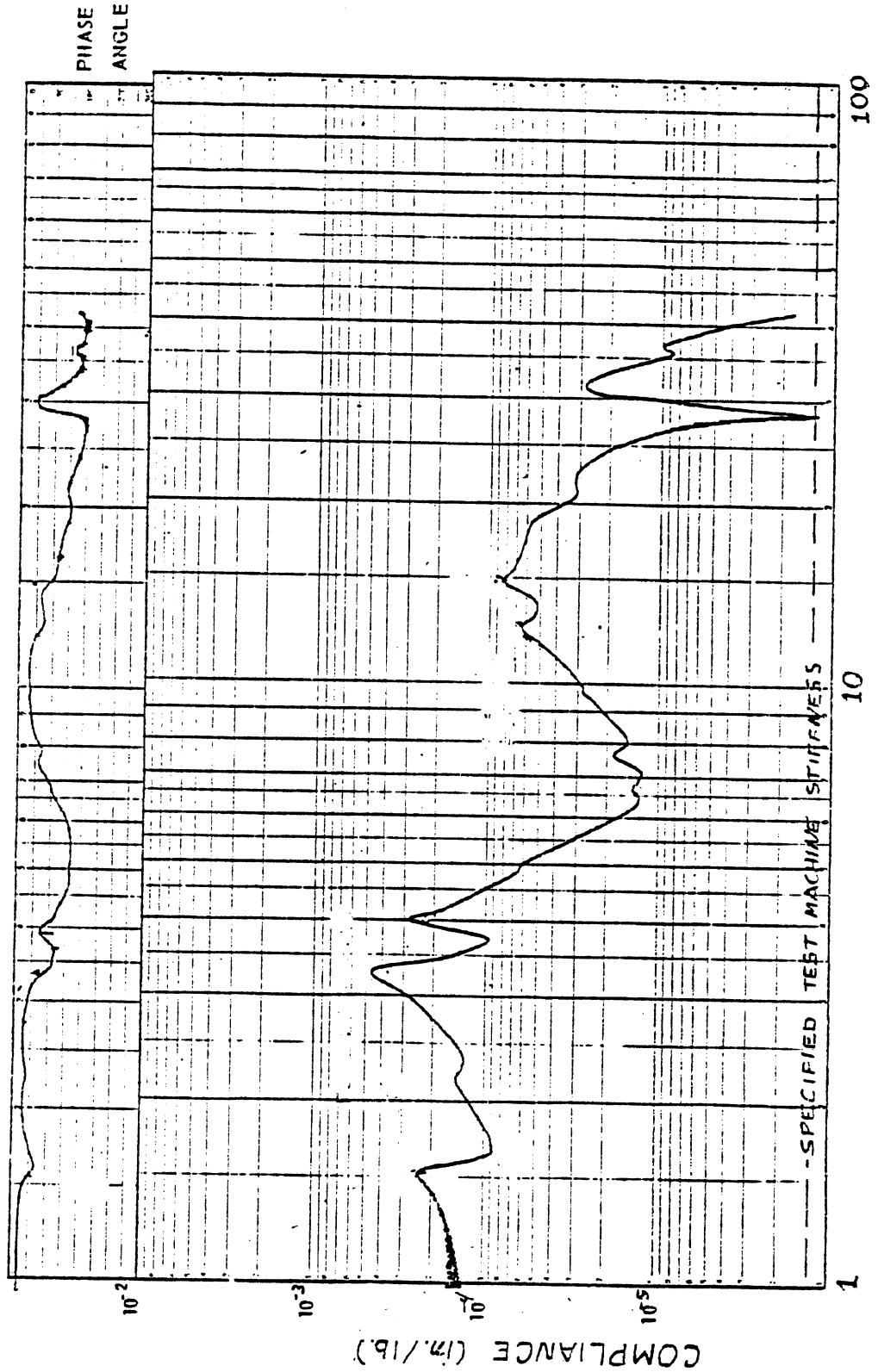

Figure 14. Driving point compliance in the vertical direction at the front axle of a highway tractor.

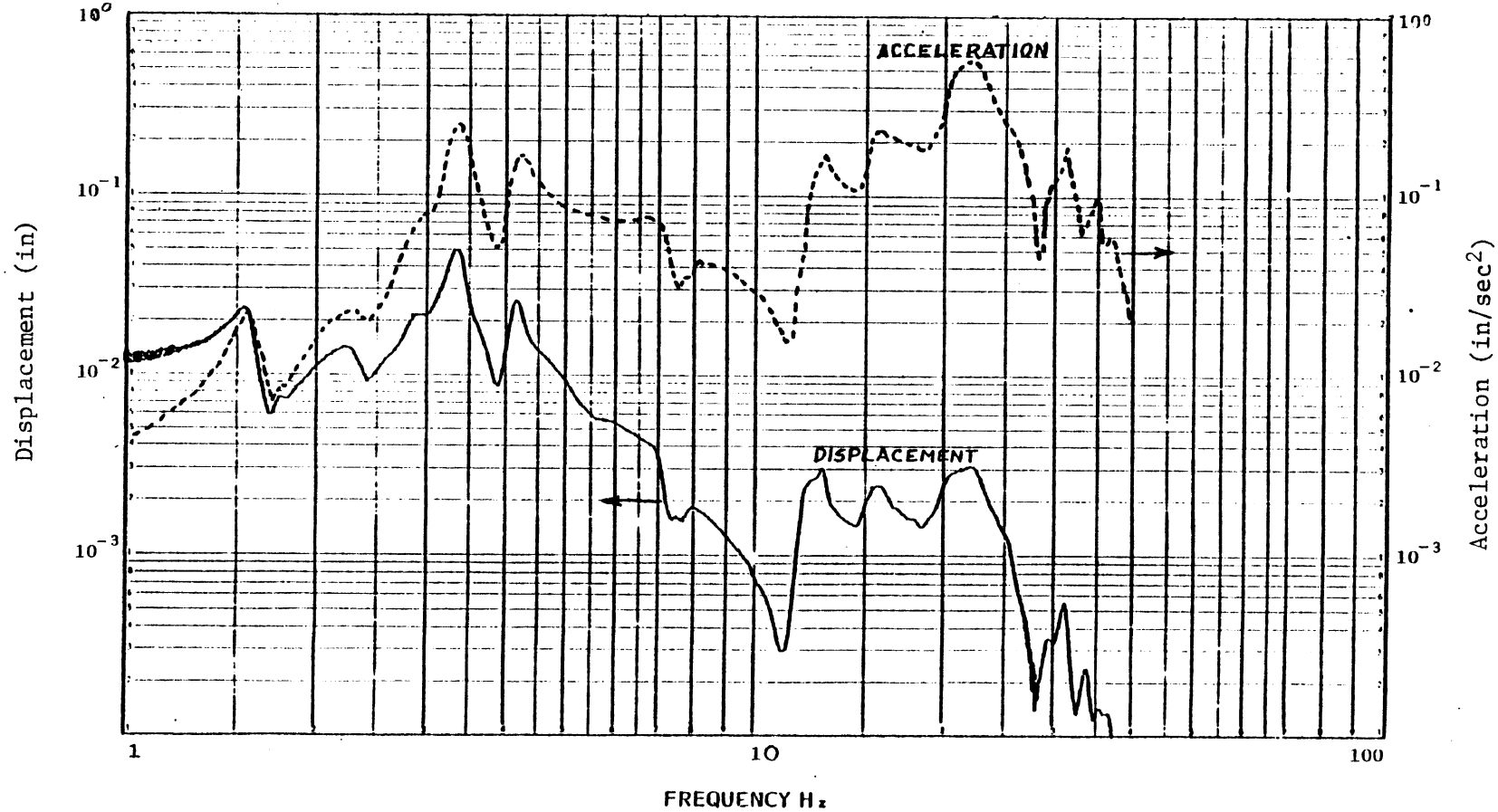

Figure 15. Vertical displacement and acceleration response on the cab of a tractor with vertical input at the front axle.

represent the most sensitive areas (most markedly at 21 Hz), it should be kept in mind that the seat tends to isolate the driver from these cab vibrations to some extent, and in addition, human tolerance of vibration is much greater at 21 Hz than at 3-5 Hz. Thus, one must view these types of measurements as informative as to the nature of vehicle response, but inadequate for really prioritizing the sensitivities of the rider. For that purpose, the direct vibration inputs to the rider must be measured at the seat/rider interface.

One last relevant mechanism to be considered in the analysis of vibration excitation by tire/wheel nonuniformities is the influence of nonlinear suspension behavior. Sinusoidal excitation at a wheel does not produce simple sinusoidal response of the sprung mass when high friction leaf spring suspensions are used. In recent studies [7], nonlinear suspension behavior was examined using the quarter-vehicle model with a comprehensive model of nonlinear leaf spring characteristics. Using a smooth road as the background spectrum on which a first harmonic tire/wheel nonuniformity excitation is imposed, the model demonstrates two interesting phenomena, which may be seen in Figure 16. In the figure, the smooth-road acceleration spectra on the sprung mass are shown with and without the superimposed wheel nonuniformity input. The addition of wheel nonuniformity input has the effect of reducing the amplitude of the response to the broadband road input, most visibly in the regions of resonance at 2 and 10 Hz. Further, the response changes in those areas of the spectrum are very significant, being an order of magnitude or more, and are thus not trivial in the characterization of the vehicle. Secondly, though the nonuniformity input is a pure sine wave excitation at 7.3 Hz, the sprung mass experiences a strong third harmonic (22 Hz) of that input due to the distortion of the waveform as it is transmitted through the nonlinear suspension. In this case, the third harmonic amplitude is only about one percent of the primary input; however, on an actual vehicle with high modal response at this frequency (as was seen in Fig. 15), a much stronger third harmonic would appear.

As Figure 16 would indicate, characterizing the response of a dynamic system with gross nonlinearities is not as simple as the familiar techniques

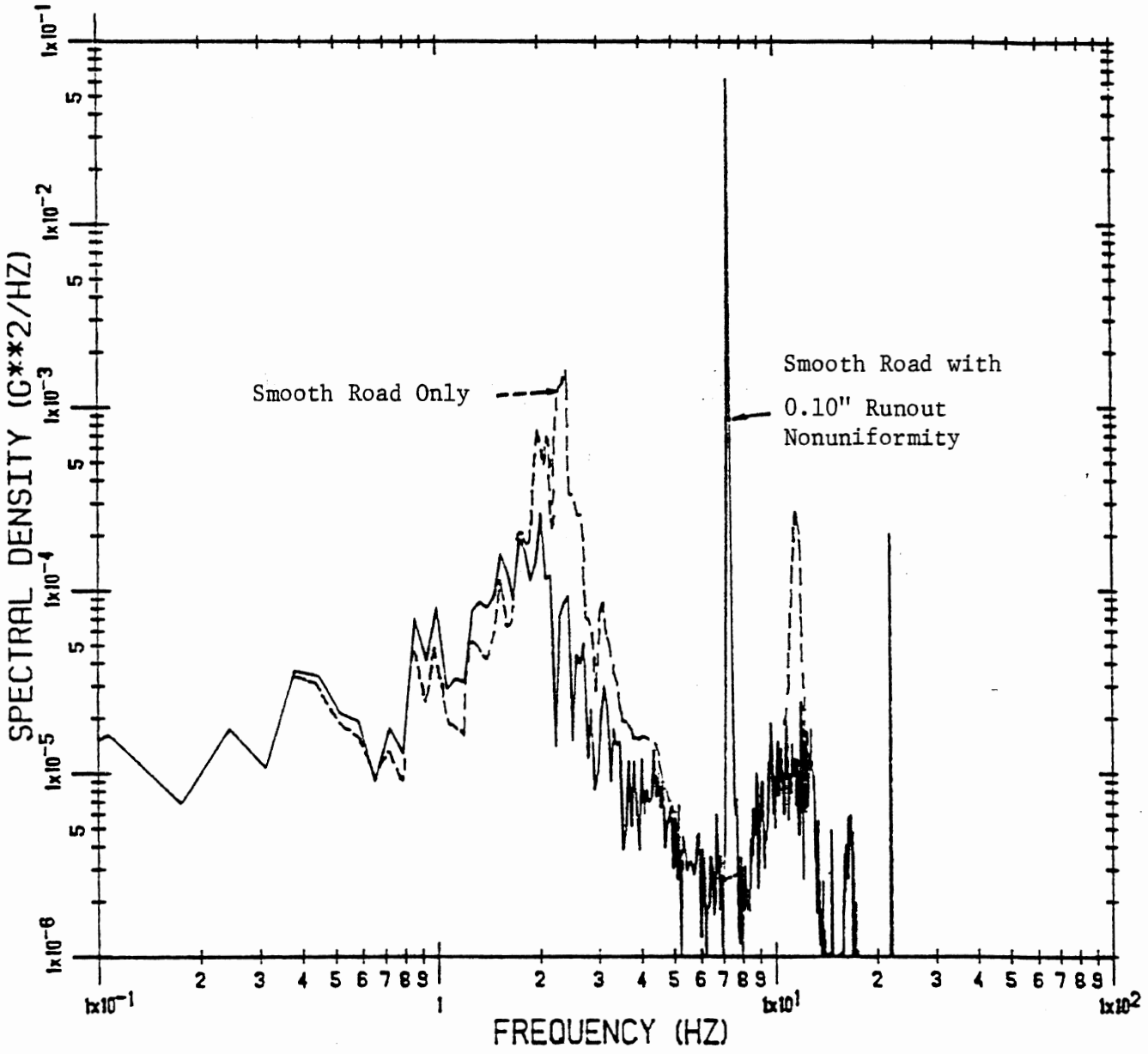

Figure 16. Acceleration spectra on a simulated vehicle with nonlinear springs operating on a smooth road, with and without tire/wheel non-uniformity effects.

used with linear systems. Nonlinearities distort the motion such that excitation in one area of the frequency spectrum adds to the response in another area. Thus, low frequency wheel inputs can result in high frequency sprung mass vibrations. In addition, the suspension damping obtained is a function of the overall spectrum of the input. Thus, the vehicle response (i.e., a transfer function) is not unique, but varies with the amplitude and spectrum of the excitation, and simple representations of truck response behavior such as shown in Figures 14 and 15 may not closely replicate on-road behavior.

4.3 Conclusions

The development of a wheel/vehicle model as done here helps to establish a systematic understanding of the dynamic system as a basis for technical communication on the subject. The analysis further leads to several conclusions to guide research on the phenomena which may be summarized as follows:

1) The nonuniformity in a tire/wheel assembly is best characterized by the force magnitude exerted against a fixed spindle while the wheel is rolling at normal operating conditions. That nonuniformity force, F_w, is the excitation force acting at the hub of a vehicle on which the assembly is mounted. The force is analogous to an external excitation force applied to the hub, but differs from the actual force produced at the axle as a result of the vehicle's response to the excitation.

2) The dynamic coupling of the nonuniform tire/wheel assembly to a vehicle, and the vibration response obtained on the vehicle, can be characterized by the combination of three complex functions according to Equations (27), (29), (30), and (31). The three complex functions are:

- -The driving point modulus at the hub of the tire/wheel assembly, D_w
- -The driving point modulus at the spindle or axle of the vehicle, D_A
- -The transmissibility from the spindle/axle to the point of interest on the vehicle, D_T.

3) The characterization of a vehicle's sensitivity to force excitation by tire/wheel nonuniformities can be accomplished in a valid manner by measuring the vibration response at the point of interest to force excitation imposed at a wheel hub. In this kind of experiment, the accuracy of the results will depend on the degree to which the wheel modulus, axle modulus, and transmissibility duplicate those of the operating vehicle. For those vibration modes which involve nonlinear elements of the vehicle (such as the vertical response modes involving deflections of leaf spring assemblies), the response behavior is dependent upon the amplitude or level of the overall excitation input. Thus, to determine the characteristic response properties for these modes, a random road input with appropriate amplitude and spectral properties should be used.

5. REFERENCES

1. Shock and Vibration Handbook. Second Edition, C.M. Harris and C.E. Crede, Editors, McGraw-Hill Book Company, Chapter 10, 1976.

2. Potts, G.R., et al. Tire Vibrations. Tire Science and Technology, Vol. 5, No. 4, 1978, pp. 202-225.

3. Dunn, J.W., et al. Rolling Tire—Vehicle Dynamic Analysis. Dynamic Analysis of Vehicle Ride and Manoeuvering Characteristics, Symposium, 28-30 November, 1978, London, England, 14 p.

4. Mills, B. and Dunn, J.W. The Mechanical Mobility of Rolling Tires. I. of Mech. Engrs. Paper C104/71, 1971, 12 p.

5. Gillespie, T.D. Validation of the MTS Model 860 Tire Test Machine Measurements. Letter report to Gary Rossow (MVMA) and Frank Timmons (RMA), March 25, 1982, 42 p.

6. Tentative Performance Specifications (5/29/79), MTS Truck Tire/Wheel Test System. University of Michigan Transportation Research Institute, May 29, 1979, 4 p.

7. Sayers, M. and Gillespie, T.D. The Effect of Suspension System Nonlinearities on Heavy Truck Vibration. Proceedings of 7th IAVSD Symposium on Dynamics of Vehicles on Roads and Tracks, Cambridge, England, September 1981.

8. Klamp, W.K., et al. Higher Orders of Tire Force Variations and Their Significance. SAE Paper No. 720463, 1972, 8 p.